GEANT-4 SIMULATION FOR SPACE BASED GeV DETECTOR

M.Tech Thesis

By

AMAN DUBEY

DEPARTMENT OF ASTRONOMY, ASTROPHYSICS AND SPACE ENGINEERING

INDIAN INSTITUTE OF TECHNOLOGY INDORE

May, 2025

GEANT-4 SIMULATION FOR SPACE BASED GeV DETECTOR

A THESIS

Submitted in partial fulfillment of the
requirements for the award of the degree
of

Master of Technology

by

AMAN DUBEY

DEPARTMENT OF ASTRONOMY,ASTROPHYSICS AND SPACE ENGINEERING

INDIAN INSTITUTE OF TECHNOLOGY INDORE

May, 2025

INDIAN INSTITUTE OF TECHNOLOGY INDORE

CANDIDATE'S DECLARATION

I hereby certify that the work which is being presented in the thesis entitled **GEANT-4 Simulation of Space based GeV detector** in the partial fulfillment of the requirements for the award of the degree of **MASTER OF TECHNOLOGY** and submitted in the **DEPARTMENT OF ASTRONOMY, ASTROPHYSICS AND SPACE ENGINEERING, Indian Institute of Technology Indore**, is an authentic record of my own work carried out during the time period from **July 2023 to May 2025** under the supervision of **Dr. Amit Shukla, Associate Professor, IIT Indore.**

The matter presented in this thesis has not been submitted by me for the award of any other degree of this or any other institute.

Aman Dubey

13/05/2025

Signature of the student with date
(AMAN DUBEY)

This is to certify that the above statement made by the candidate is correct to the best of my/our knowledge.

13-05-2025

Signature of the Supervisor of
M.Tech. thesis (with date)
(Dr. AMIT SHUKLA)

AMAN DUBEY has successfully given his/her M.Sc. Oral Examination held on **05/05/2025**.

Signature(s) of Supervisor(s) of M.Tech thesis
Date: **13/05/2025**

Programme Coordinator, M.Tech.
Date: 16-05-2025

Manoneeta Chakraborty
Convenor, DPGC
Date: 16/05/2025

HoD, DAASE
Date:

ACKNOWLEDGEMENTS

I am truly grateful to my advisor, Dr. Amit Shukla, for his continuous support, encouragement, and thoughtful guidance throughout this work. Our many meaningful discussions have deepened my understanding and helped me grow as an independent researcher. His patience, insightful feedback, and constructive suggestions at various stages of the project were incredibly valuable.

I am also thankful to the Department of Astronomy, Astrophysics, and Space Engineering, IIT Indore, for providing the atmosphere and essential resources for carrying out this project.

I am thankful to Dr. Satyajit Jena for his valuable guidance at the beginning of this project. I learned a lot about different aspects of GEANT-4 simulations, which is an integral part of my thesis. I am grateful to him for his support and encouragement while learning the simulations.

I gratefully acknowledge Dr. Indranil Das, Dr. Sujay Mate, and Dr. NPS Mithun for their contributions to help me in understanding the GEANT-4 framework. I have benefited a lot from their work and discussions with Dr. Indranil Das and suggestions from Dr. Sujay Mate, particularly about Geometry and Physics implementation techniques in GEANT-4, were very helpful for this project.

A special thanks goes to my labmates, Chandan Bhai and Ayush Bhai, for their suggestion at different stages of the project and the fruitful discussions we had, which led me to think about my ideas from a different perspective. I am grateful to them for being with me when I am down because their encouraging thoughts help me to start over. A special thanks to Hari, Daisy, Shraddha Di, and Sushmita Di for many fruitful discussions on several topics of physics, which led me to understand it better. I extend my deepest appreciation to my friends Eeshan, Rajat, Abhishek, Sana, Tejas, Ranjan, and Sourdeep. Your unwavering support at all times has made this journey more enjoyable and less daunting.

Finally, I am deeply grateful to my parents and the rest of my family members for their constant support in my life. I especially thank my elder brother-cum-best friend Munendra for being so supportive all the time, and I am indebted to him for his support in my every high and low over the past years.

Abstract

The thesis presents an extensive analysis of the modeling of a space-based GeV detector, using the GEANT-4 toolkit. The main goal is to develop and verify a detection system to identify and characterize high-energy particles in space, emphasizing precise position hits & energy deposition measurements. This research is driven by the need for sophisticated detection systems in space missions focused on investigating γ rays.

The GEANT-4 simulation framework is used to simulate the physical processes and interactions of particles with detector materials. The detector design includes an anti-coincidence and tracking module for accurate hit positions and energy deposition measurements.

The study includes the thorough layout of the detector geometry, the execution of primary particle creation, and the simulation of particle interactions. The thesis incorporates the analysis of a simulated model for the hits and the energy deposition measurement.

The results indicate the detector's ability to detect the particles coming onto it by specifying the coordinates where they hit the detectors, precisely quantify the energy of arriving particles, and furnish dependable data for subsequent scientific investigation. This study advances the construction of space-based detectors, which will be more sophisticated and improve our understanding of high-energy particle environments in space.

This work demonstrates the versatility and efficiency of the GEANT-4 toolkit in detector simulation while offering significant insights for future space missions and the progression of space-based high-energy particle detection technology.

Contents

List of Figures

Chapter 1

Gamma Ray Astronomy: Introduction

1.1 Background

The exploration of the universe beyond the visible range, starting from Radio to X-rays and $\gamma-$rays, led humans to explore the universe in all ranges of wavelengths of the electromagnetic spectrum. Every wavelength regime has mysterious phenomena, clouding the vision until years of effort by the community to understand it completely. The need to understand the extreme Universe has led to the development of gamma-ray astronomy.

Gamma-ray astronomy is a discipline of observational astronomy for the detection and γ-rays. Since Gamma rays possess wavelengths shorter than $< 10^{-5}$ meter and energy surpassing 100 keV[5, 6], rendering us to investigate high-energy processes, providing insights into the behavior and characteristics of celestial objects that generate this radiation. Since they are not deflected by the galactic and intergalactic magnetic field, this provides an opportunity to unveil the most powerful particle accelerators, the surroundings of compact objects, and the dynamics of active galactic nuclei[1]. Moreover, gamma-ray observations enhance our comprehension of essential scientific processes, including nuclear reactions and matter-antimatter interactions. Gamma rays possess significant energy, enabling them to traverse most materials, hence challenging detection and analysis. This penetrating capability also enables them to furnish information on dense and otherwise impenetrable astrophysical sources.

1.1.1 The Physics of Gamma-rays of the Universe

To understand the Universe in the gamma-ray domain, let's assume our eyes as gamma-ray detectors and try to see around. We will see nothing except some rare flashes of gamma-ray light. The reason behind this is : (i) Gamma- rays are quite a rare event on Earth, and (ii) most gamma-rays do not reach Earth because of the natural shield of the Earth's atmosphere[1]. Now imagine yourself beyond the Earth's atmosphere. Then, you will see a gamma-ray sky with a

bright diffuse line corresponding to the Milky Way, with thousands of point-like bright variable spots filling the whole celestial sphere. The gamma-ray sky is represented in Figure 1.1:

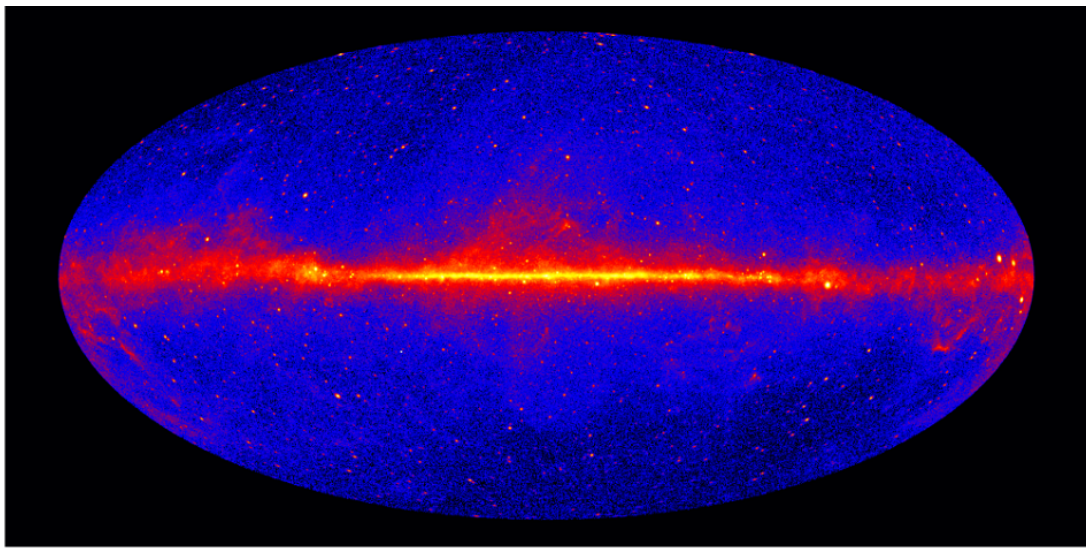

Figure 1.1: The Gamma-ray sky map by Fermi's LAT. Credit: NASA/Fermi LAT Collaboration.

NOTE: The image above is a small portion of the gamma-ray sky which is covered by the instrument onboard on Fermi satellite covering a large energy band.

1.1.2 Gamma-ray band of electromagnetic spectrum

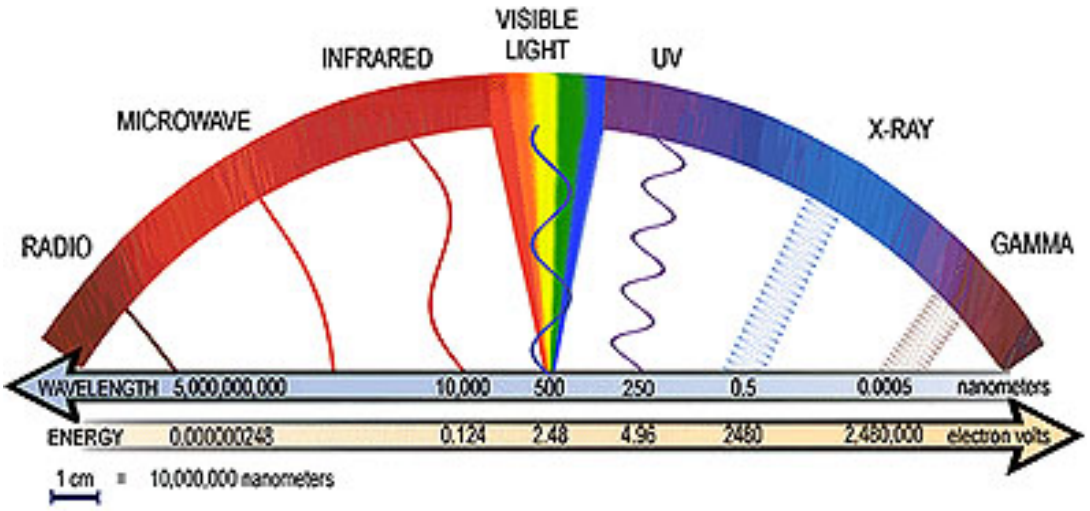

Figure 1.2: Electromagnetic representation: Schematic representation[1].

Figure 1.2 shows schematics of the electromagnetic spectrum in which gamma-rays lie on the upper right end of it. In astronomy, the energy of gamma rays is defined as $> 10^5$ eV. The largest energy photon ever detected for gamma-rays is in the PeV order[7]. This leads to the conclusion that the gamma-ray energy band lies from 10^5eV to 10^{15}eV approximately, which makes it the most variable band of the EM spectrum and also the most varied in terms of emission mechanisms and detection techniques.

Due to the wide range of energy bands for gamma-rays, we defined specific intervals of bands in which different detector mechanisms with different detector types operate. For example: The low energy band lies in between 100keV - 30MeV range, where the dominant mechanism is Compton scattering and the detector type is balloon or satellite. The high energy range lies between 30 MeV - 100 GeV, where Pair production dominates for the detector mechanism, and the detector is onboard a satellite[6]. At higher energies, the detection is ground-based. For eg, at Very High energy (100GeV-30TeV), the mechanism is Atmospheric Cherenkov, and the detectors are ground-based[6]. Similarly, for Ultra High energy (30TeV - 30PeV), the detector mechanism is Water Cherenkov, and detectors are ground-based[1, 5].

1.2 Origins of Gamma Rays

The main sources of the gamma-rays are emission from galactic and extragalactic objects. The study of emissions from these sources helps to investigate several astrophysical mysteries of the universe.

1.2.1 Galactic Sources

The prominent galactic sources for the gamma-ray emission are supernova remnants, pulsars, and high-mass X-ray binaries. A brief introduction to these sources is given in the upcoming sections:

(i) Supernova Remnants (SNRs)

The explosion of a big star emits an immense quantity of energy ($\approx 10^{51}$ ergs), including radio, X-ray, and gamma rays (GeV to TeV range). They are also the predominant source of galactic cosmic rays because of the diffuse shock acceleration mechanism of charged particles[8]. The production of gamma-rays in the shell-type supernovae remnants, where the remnant material exists in the form of several shells, are because of extremely energetic electrons via process of synchrotron, bremsstrahlung, or inverse-compton process. The evidence shows acceleration of protons, and it can lead to the detection of gamma-rays because of the decay of neutral pions, which are produced by the interaction of protons with the interstellar medium. The electron

acceleration for energy $> 10^{12}$ eV in SNRs comes from X-ray studies of SNRs[9, 10].

(ii) Pulsars

Pulsars are rapidly revolving neutron stars. Many pulsar wind nebula shows the signature of emission of gamma rays from them[11]. In a pulsar wind nebula, a pulsar is surrounded by a supernova remnant, and the nebula is powered by the pulsar. The loss of rotational energy in a pulsar is due to streaming winds of positrons, electrons, and ions. These winds are stopped by the nebular materials, leading to a wind shock front (collisionless shocks), where no loss of energy will happen if the particle interacts with the shock front[8]. If we look at any typical pulsar wind nebula models, the particles in winds (electrons & positrons) are accelerated by the magnetohydrodynamics process before they are stopped by the wind shocks. Then they are further accelerated to even higher energies through the Fermi acceleration mechanism in the random downstream region of the shocks[12], and then they are streamed into the surrounding nebula. Within the nebula, they interact with the magnetic fields and photon fields, and matter to produce gamma-ray photons via inverse Compton, bremsstrahlung, and synchrotron processes.

(iii) Binary Systems

Systems including a neutron star or black hole that accrete materials from a A companion star can generate gamma rays via mechanisms such as inverse Compton scattering[13].

1.2.2 Extragalactic sources

The prominent extragalactic sources emitting the gamma-rays are Active Galactic Nuclei, Gamma Ray Bursts, etc. A brief introduction to these sources is given in the upcoming sections:

(i) Active Galactic Nuclei (AGN)

AGN can produce very luminous radiation from the compact volume, making them the most prominent source for TeV gamma-ray emission. AGNs host supermassive black holes, located at their center, and it is accreting materials from the surrounding and release a large amount of gravitational energy. The emitted energy is due to both thermal and nonthermal processes; the former comes from the accretion disc, and the latter comes from jets of relativistic particles emanating perpendicular to the plane of the disc[14].

The acceleration of particles happens in jets even beyond the host galaxy. These particles interact with the magnetic field and ambient photons, giving emission due to synchrotron and inverse Compton processes. The TeV gamma-ray emitters for AGNs come from an interesting class of AGNs known as blazars[15, 16].

1.3 Obstacles in Gamma Ray Detection

Detecting gamma rays is associated with several notable challenges.

1.3.1 Earth Atmosphere Interaction

Gamma rays are absorbed by the Earth's atmosphere, which generally inhibits their detection. This is because of the transparency of the Earth's atmosphere, as it acts as a shield for the radiation coming from outer space[6]. Thus, direct detection can only happen in the high atmosphere with the help of satellites[1]. For the very high energy range (> 100 GeV), gamma-ray propagation creates so disturbing effects that can be recorded from the ground-based instrument, leading to their indirect detection.

1.3.2 Low Flux and High Energy

Gamma-ray sources typically exhibit a low photon flux, indicating that the quantity of gamma rays detected per unit area is minimal.

1.3.3 Background Radiation: Cosmic Rays

Detection of gamma rays is complicated due to contributions from multiple sources, such as cosmic ray background[17] and the noise from the detection instrument itself[4]. The major contribution comes from cosmic rays as it spans to energy range from 10^6eV to 10^{20}eV. The cosmic rays consist mainly of protons, a fraction of electrons, and other particles. The main source of cosmic rays is supernova remnants, which can also emit gamma rays. These accelerating protons in cosmic rays can generate gamma-rays by inverse Compton and bremsstrahlung processes, but their gamma-ray spectrum will be a little different from that of electrons, thus leading to a challenge of precise detection of gamma-rays with background as cosmic rays.

1.3.4 Precise Detection

Gamma-ray telescopes utilize indirect techniques like pair production for detection. Thus, we need highly sensitive and precise instrumentation[4].

1.4 Interaction mechanism

Gamma rays engage with matter via different processes, each offering distinct insights into astrophysical phenomena. Since we are focusing on space-based detectors, they mainly interact with matter via Compton scattering or by pair production.

1.4.1 Compton Scattering for gamma-rays

This method is employed to identify gamma rays throughout the medium-energy spectrum (1 MeV to 30 MeV)[1]. This process happens when a gamma photon interacts with a loosely bound or free electron, leading to partial energy transfer from the photon to the electron, accompanied by a modification in the photon's direction and energy. Compton scattering includes the inelastic collision between a gamma-ray photon and an electron. Due to Compton scattering, the wavelength of a photon will get changed, which is given by the equation

$$\boxed{\Delta\lambda = \lambda_c[1 - cos(\theta)]} \tag{1.1}$$

where $\Delta\lambda$ = change in the wavelength of the photon.
$\lambda_c = \frac{h}{m*c}$= Compton wavelength for the material particle.
m = rest mass of material particle c= speed of light.

The energy of the scattered photon E'_γ can be expressed as:

$$\boxed{E'_\gamma = \frac{E_\gamma}{1 + \frac{E_\gamma}{m*c^2}(1 + cos(\theta)}} \tag{1.2}$$

where E_γ is energy of incident photon.

1.4.2 Pair Production in Gamma Ray Interactions

Pair production is a fundamental interaction mechanism for high-energy gamma rays, especially for photons with energies exceeding 1.022 MeV. This process happens when a gamma-ray photon interacts with the electromagnetic field of a nucleus, resulting in the conversion into an electron-positron pair.

The interaction generally occurs near a nucleus, which absorbs a portion of the momentum to maintain energy and momentum conservation throughout the process. The equation for the pair production:

$$\boxed{\gamma + \gamma \Longrightarrow e^+ + e^-} \tag{1.3}$$

1.5 Gamma Ray Detection

Detecting gamma rays is difficult because of their enormous energy and penetrating characteristics. Before starting with the detection technique, we need to understand the behaviour of the transparency of the atmosphere. As the atmosphere acts as a shield for us from high-energy

radiation from outer space, it absorbs most of it except a tiny window of the optical wavelength range and radio regime[1]. Thus, we can conclude that the direct detection of gamma rays is possible at high altitudes or in outer space, using satellites[6]. For gamma-rays whose energy is $> 100GeV$, they can produce disturbances while passing through the atmosphere, and the effects of these disturbances can be recorded by the ground-based instrument[5], leading to their indirect detection that uses our atmosphere as part of the detector. The whole idea mentioned here is summarized below in Figure 1.3:

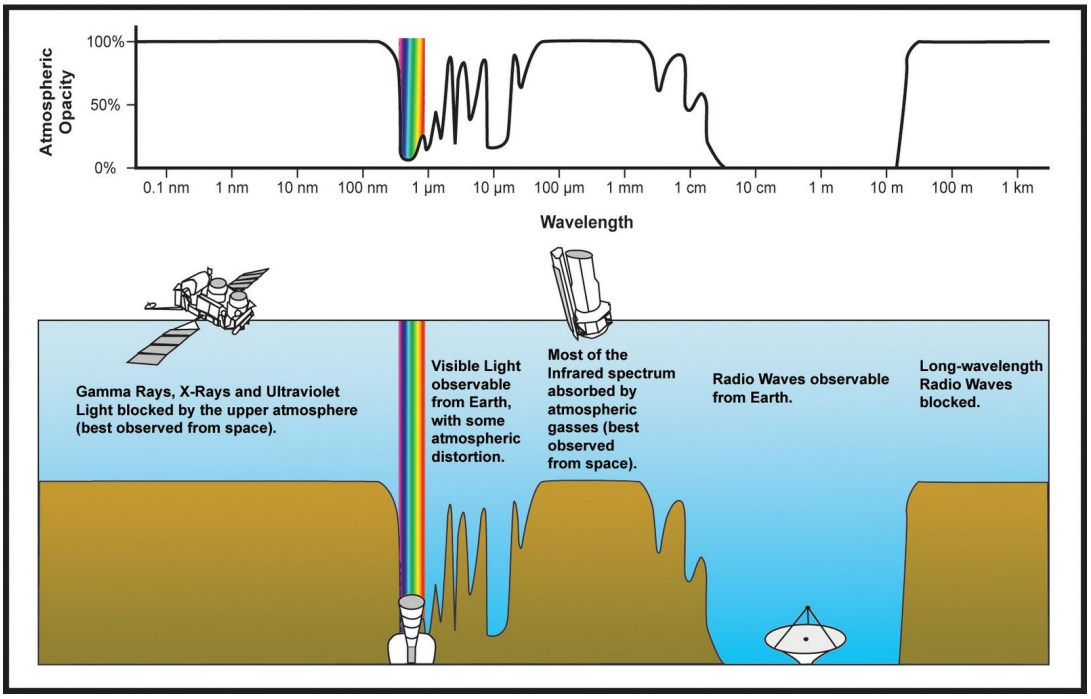

Figure 1.3: Opacity/transparency of Earth's atmosphere for different wavelengths[1].

Thus, to design a new gamma-ray detector we need to take care about the following things for eg: identifying large number of photon with good spatial and energy resolution with good sensitivity, determining the direction of arrival with good angular resolution with $24 * 7$ patrol to large portion of the sky for large field of view. An ideal detector has all these things simultaneously, i.e, it has excellent sensitivity, good angular and energy resolution with a wide field of view. But in reality, we need to compromise to keep one aspect for the other, depending on the needs. Thus, we can conclude that detecting gamma-rays means we are estimating **their incoming direction, energy, and time of arrival[1].**

The usual detection of photons is done by reflecting them and then concentrating them in a particular area of sensitive detectors, but for high-energy photons, it's difficult to divert them from their initial path. Thus, their detection technique comes from particle physics detectors.

The technique of particle physics detectors for gamma-ray detection is incorporated in two different ways: (i) Space-based detection. (ii) Ground-based detection.

Both techniques have their own challenges, but technological development that can withstand the limitations helps us to achieve this.

1.5.1 Space-Based Detection

The Space-Based detection involves space-borne detectors in the form of satellites. Effectively, to measure gamma-ray photons, we need to convert a part of their energy to the energy of electrons, released from the medium itself. The interaction mechanism of the particle depends upon the energy of the primary photon[1], and mainly we have to deal with three processes known as photoelectric, Compton, and pair-creation effects. Figure 1.4 shows the variation of the mass attenuation coefficient for a photon with energy from the keV to MeV range. From this, we can conclude that the predominant process for the low energy is the photoelectric effect, around 1 MeV, the predominant process is the Compton effect, and for a few MeV to other high-energy range, electron-positron production is dominated.

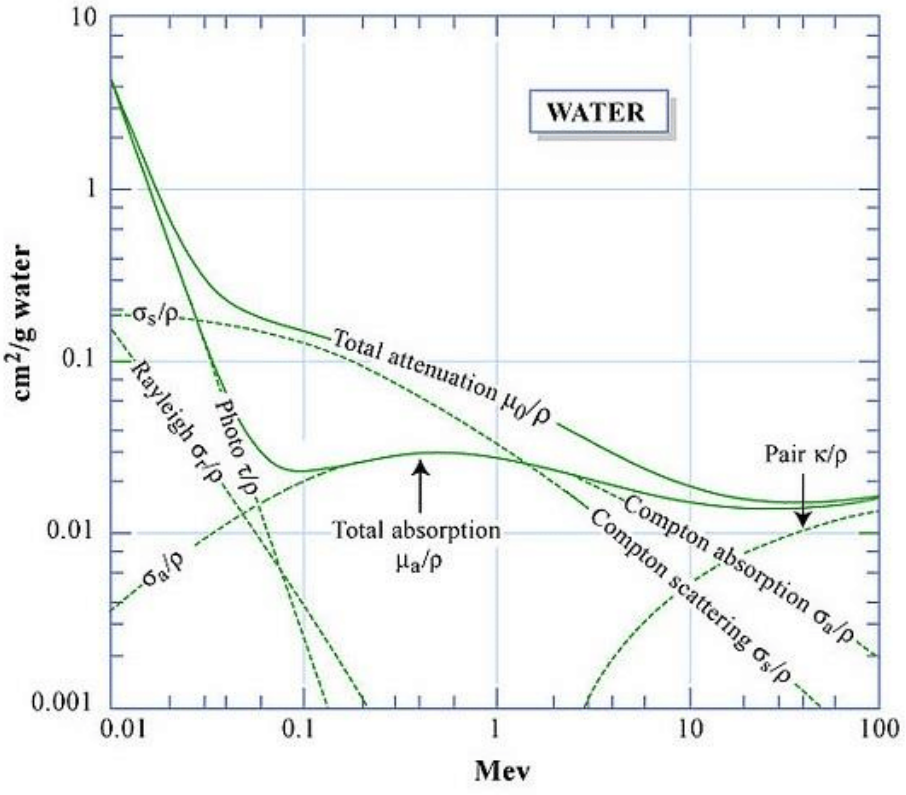

Figure 1.4: Mass attenuation coefficient for photons in water and interaction happening for different energy ranges[1].

For space-based detection, the first challenge for us is to tackle background radiation, which contains mostly cosmic rays. Therefore, any gamma-ray satellite should have first an anti-coincident shield (ACD)[4, 18]that surrounds the gamma-ray detector to prevent passage of the charged particle. Since we are interested in photons, all things remain a background for us, and these signals are rejected. The main part of the detector contains the tracker module, which helps to identify gamma-rays and can be helpful to do reconstructing tracks and the incoming direction[4]. The photon entering here will be converted to a charge particle and then converted to an electric pulse, recorded by the onboard electronics instrument. The other module, called a calorimeter, will record the energy of the particle via a scintillation mechanism. Also, they will have a power supply, so they need solar panels, and for data transmission, we have the antenna mounted on it with DAQs (Data acquisition system)[4].

The interaction mechanism for the space-based detector depends on different energy regimes of incoming particles, which leads to the classification of space-based detectors. The upcoming section explains the detectors based on these mechanisms:

(i) Compton Detectors

If the energy of the photon lies in the MeV regime, the dominant process is the Compton effect. Figure 1.5 shows a Compton detector's schematic representation. These types of detectors have two detector systems: the first detector will scatter the incident photon, and the second one will absorb it.

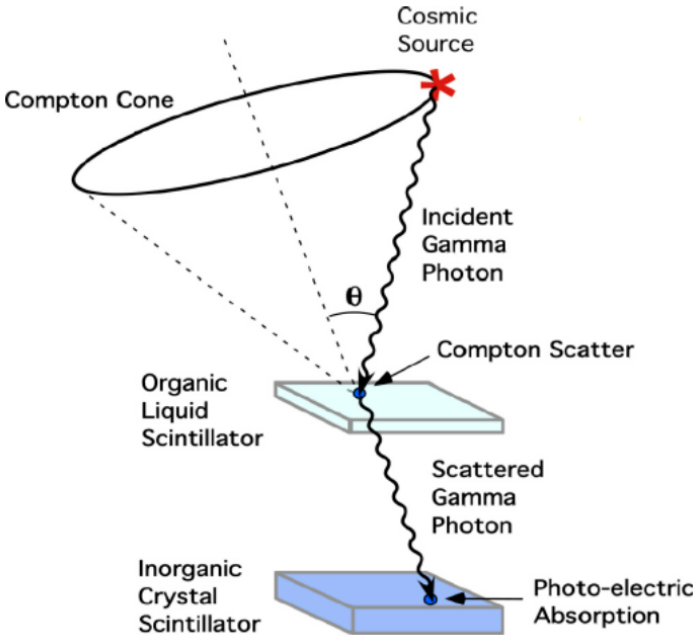

Figure 1.5: Compton detector schematic representation.[1]

If the energies of incoming photons in two detectors are, say, E_1 and E_2, the angle of scattering θ is given as:

$$\boxed{cos\theta = 1 - (\frac{m_e c^2}{E_2}) + (\frac{m_e c^2}{E_1 + E_2}} \tag{1.4}$$

The Compton detectors have a large field of view, but their sensitivity is low in comparison to other instruments. An example of Compton detectors is CGRO.

(ii) Pair Production Detectors

Here, incoming gamma rays generate electron-positron pairs upon interaction with matter. This dominates in the energy regime of 100 MeV to 100 GeV. They have a high Z material element, which will enhance the probability of pair production. After the creation of the pair, it will penetrate the detector, allowing its path to be tracked. At the end, a calorimeter is located to measure the energy. A prominent space-based telescope based on pair production: Fermi Gamma-ray Space Telescope[4]. The details regarding this will be explained later.

1.5.2 Ground Based Detection

For the ground-based detection, gamma-rays will have to interact with atmospheric nuclei, so a direct detection mechanism like a space-based detector can't work here. The interaction of a photon with the atmosphere will initiate multiple process that converts the photon to low-energy photons, electrons, and positrons, leading to an extensive atmospheric shower (EAS)[1, 19].

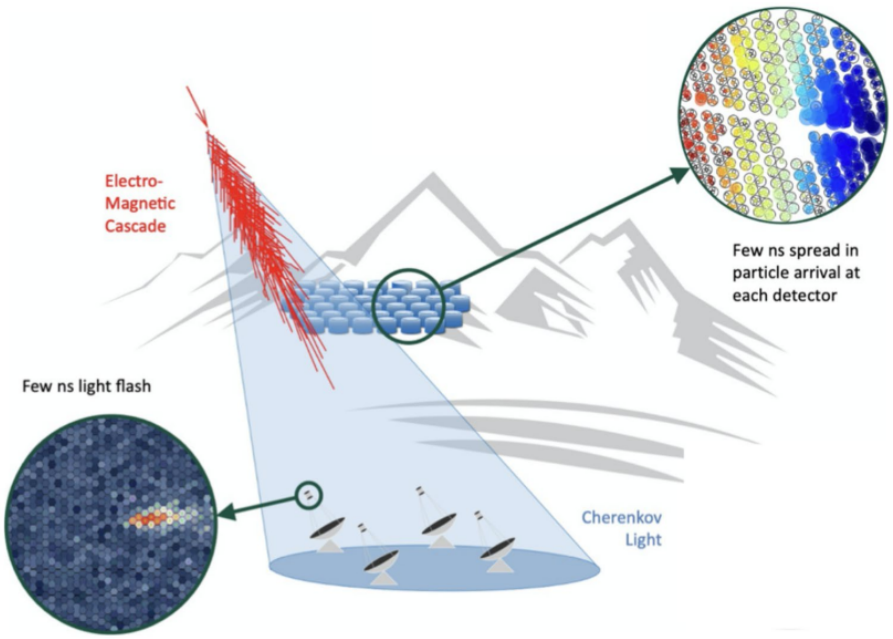

Figure 1.6: Ground based detection method for the gamma-ray photons[2]

These showers are measured directly at a few altitudes above the ground. The Secondary radiation in the UV-visible regime photons known as Cherenkov radiation, penetrates the inner layer and reaches the ground, and is detected by the ground-based instrument[1].

(i) EAS Mechanisms Detectors

These types of detectors are located at higher altitudes for the detection of charged particles in the EAS shower[19]. After the first interaction of a photon with the nucleus, it gets converted to an electron-positron pair. The electrons produce photons via the bremsstrahlung process, and proton produces photons via the hadronic process.

(ii) Imaging Atmospheric Cherenkov Detectors (IACTs)

The IACTs work for a few tens of GeV to TeV energy range. The detection technique is based on the detection of Cherenkov light induced by cosmic rays in the atmospheric shower[20]. In the Cherenkov effect, the charged particle travels with a speed greater than the speed of light in the given medium (dielectric). When it travels in a dielectric medium, it will polarize the medium, and when the speed of the particle is greater than the speed of light, then a coherent wavefront appears at an angle θ and emits Cherenkov radiation[1]. This radiation is detected by the ground-based detectors.

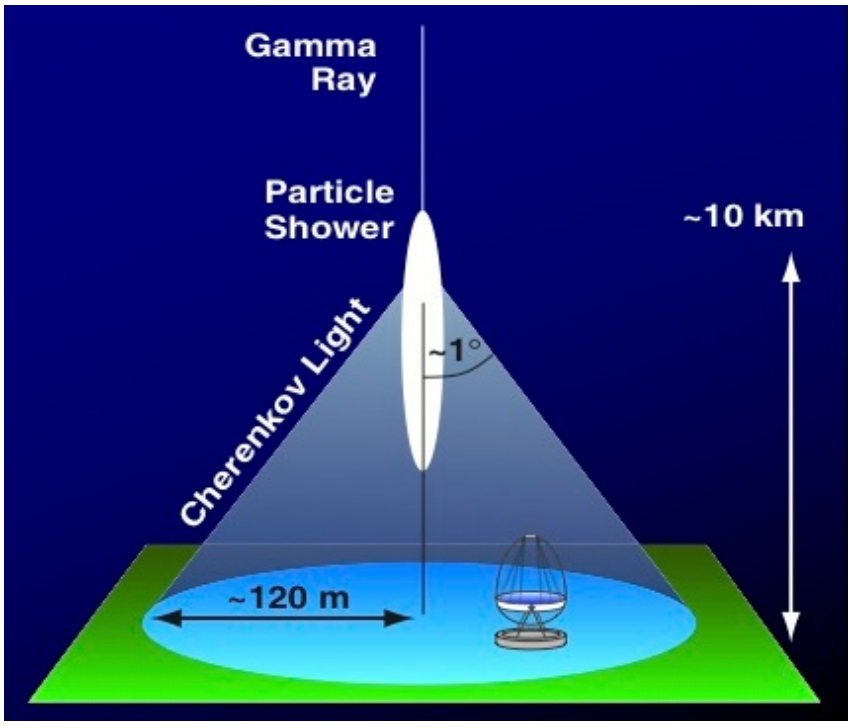

Figure 1.7: IACTs detectors: Schematics for atmospheric shower detection.[3].

Figure 1.7 explains the imaging technique to study the images produced by the Cherenkov Photons by EAS when focused on the plane. The idea of the imaging technique is to use the shape and orientation of the images to get information about the direction of arrival and the energy of the incoming photons. The prominent operating IACTs are HESS, MAGIC, FACT, etc.[1, 3].

1.6 Problem statement & Objectives

Notwithstanding these limitations, technological and instrumental developments have rendered gamma-ray astronomy a swiftly progressing discipline.

This thesis is motivated by the LAT (Large Area Telescope) of the Fermi γ-ray space mission. The LAT is predicated on the pair-production process and is engineered to measure the directions and energy of γ-rays while eliminating background interference. The aims of the investigation presented in this thesis are summarized below:

1. To emulate an ACD (Anti-coincidence Detector) and tracking module for the detection of γ-rays, utilizing the Geant-4 toolkit.

2. To record hits on the tracker module sites for particle detection, including the positional data of strikes on the detection sites.

3. To calculate energy deposition at each point for the analysis of energy loss.

1.7 Thesis Outline

The thesis outline is as follows. In Chapter 2, a concise review of the instrument's literature is provided, which underpins the motivation for the thesis investigation. In the first half of Chapter 3, we discuss the GEANT-4 toolkit and its functionality. The second half includes a discussion on the approach for constructing simulation models using GEANT4[21]. In Chapter 4, the first half discusses the results of the development of simulation for the preliminary configuration of the detector. The second half of this chapter includes the examination of the preliminary findings and the subsequent discussion of these findings. Chapter 5 presents the simulation results of the detector system having a configuration similar to Fermi LAT in the first half, where the description of geometry and physics is provided. The second half of Chapter 5 discusses the findings and subsequent discussion on them. Chapter 6 presents the summarized conclusions drawn from the work and outlines the future scope of the work linked to the current study.

Chapter 2

Literature Review

The work for the study is inspired by the Large Area Telescope (LAT) of the Fermi Mission. The following section elaborates on the description of LAT.

2.1 Large Area Telescope (LAT)

The Large Area Telescope (LAT) is a crucial tool in γ-ray astronomy, offering unparalleled understanding of high-energy events in the universe. The LAT emerged as one of the most effective and adaptable gamma-ray detectors ever utilized. The major objective is to detect γ-rays within the energy range, approximately 20 MeV to over 300 GeV, documenting the most energetic phenomena in the universe[4].

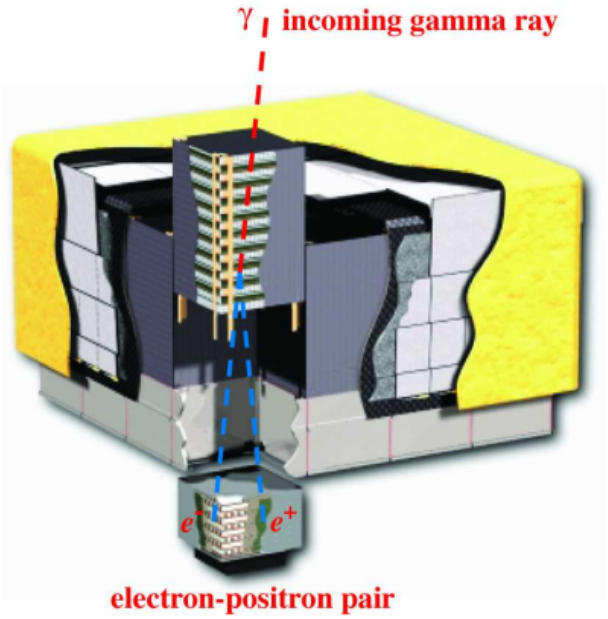

Figure 2.1: The LAT Telescope[4].

Figure 2.1 shows the LAT, which is a telescope based on the pair creation method. It utilizes high-resolution converter trackers to determine the trajectories of the incident γ-rays and a calorimeter to measure their energy while eliminating background interference. The LAT consists of sixteen precision tracker modules and calorimeter units[4]. These detectors capture the paths of the electron and positron produced during pair creation from incident γ-rays, predominantly in a thin, high-Z foil, while The calorimeter evaluates the energy of the resulting electromagnetic shower[4].

The fully assembled LAT telescope features an anti-coincidence detector designed to reduce background noise from charged particles[22]. Every tracker module consists of eighteen X-Y tracker planes, which include an array of silicon-strip detectors (SSDs) for the detection of charged particles[4]. The trackers ascertain the arrival direction, while the calorimeter located beneath them evaluates the energy. The tracker's aspect ratio (height/width) is 0.4, which facilitates a broad field of vision, allowing the majority of conversion showers to enter the calorimeter for energy measurement[4, 23].

2.2 Technical description of LAT modules

The Large Area Telescope (LAT) is made up of numerous main components, each with a significant role in detecting and interpreting gamma rays. These components work together to provide the LAT's high sensitivity, wide energy range, and precise measuring capabilities. The description of the main components of LAT is elaborated in upcoming sections.

2.2.1 Anti-Coincidence Detector (ACD)

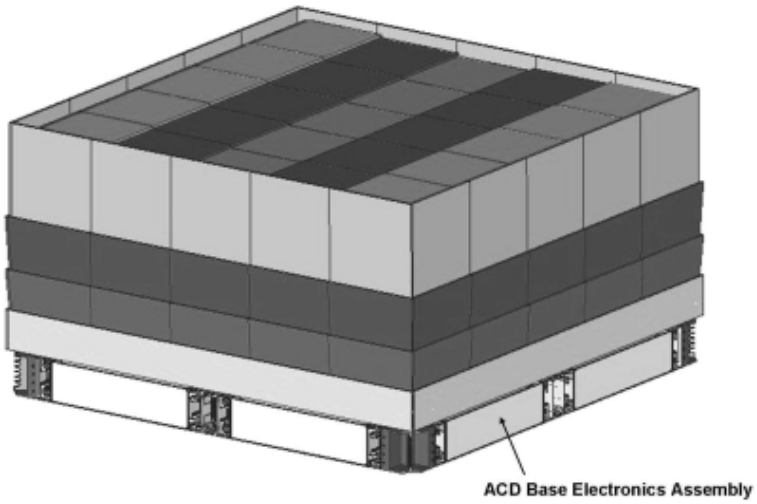

Figure 2.2: The ACD with electronics at its base.[4].

Figure 2.2 shows the ACD module for the LAT of the Fermi-Gamma Rays space mission. The ACD wraps around the tracker and calorimeter, acting like a barrier against charged particle background interference[22, 24]. The system comprises plastic scintillator tiles that identify and reject charged particles entering the LAT. This guarantees the recording of solely neutral gamma rays, hence enhancing the signal-to-noise ratio. Thus, it serves the purpose of charged-particle background rejection and event detection[4, 22].

Background rejection: Differentiating charged particles to minimize background noise.

2.2.2 Tracker Module

The tracker has been developed to ascertain the trajectory of incoming gamma rays. It comprises several layers of silicon strip detectors interspersed with tungsten foils. Upon entering the tracker, a gamma ray interacts with the silicon layers, which results in the electron-positron pair.

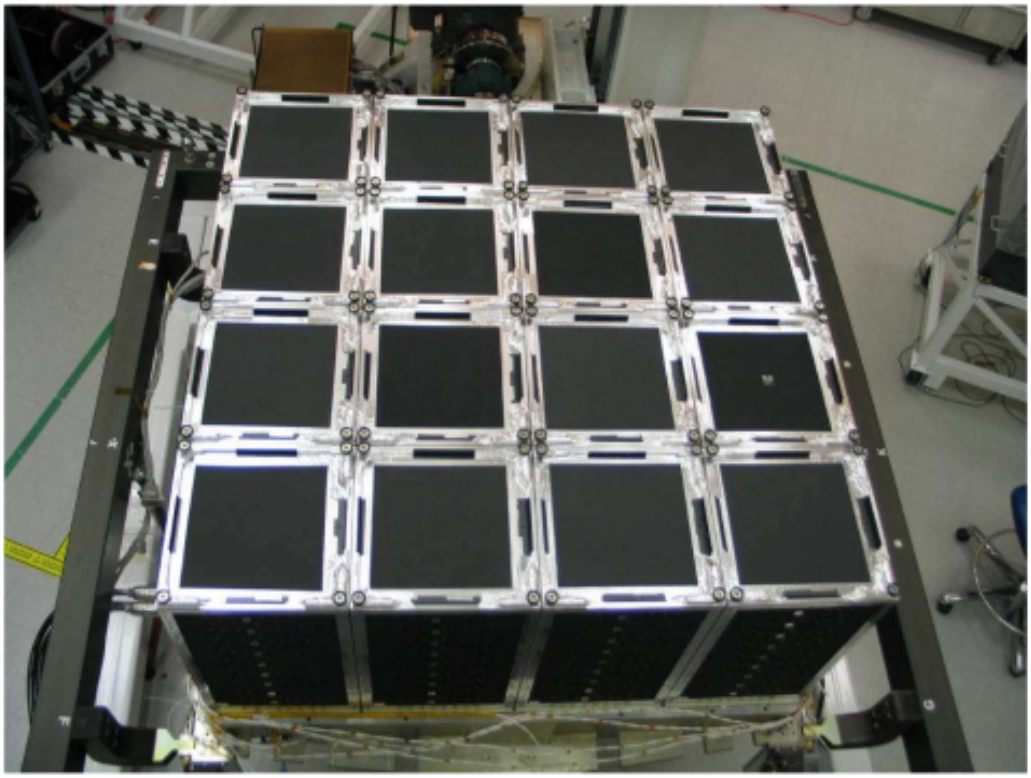

Figure 2.3: The tracker array of LAT[4].

For recording the path of particles, position-sensitive detectors are placed between interleaved planes[4]. These position-sensitive detectors are arranged in a crossed form of strips to

cover all directions[23]. The silicon strip detectors subsequently ascertain the trajectories of these particles, facilitating the reconstruction of the initial gamma ray's direction. The tracker's readout circuits are configured to operate with a single threshold level, storing only 0 or 1 for each channel hit When a trigger is activated. Consequently, the system can achieve low deadtime with minimal noise[4].

2.2.3 Calorimeter

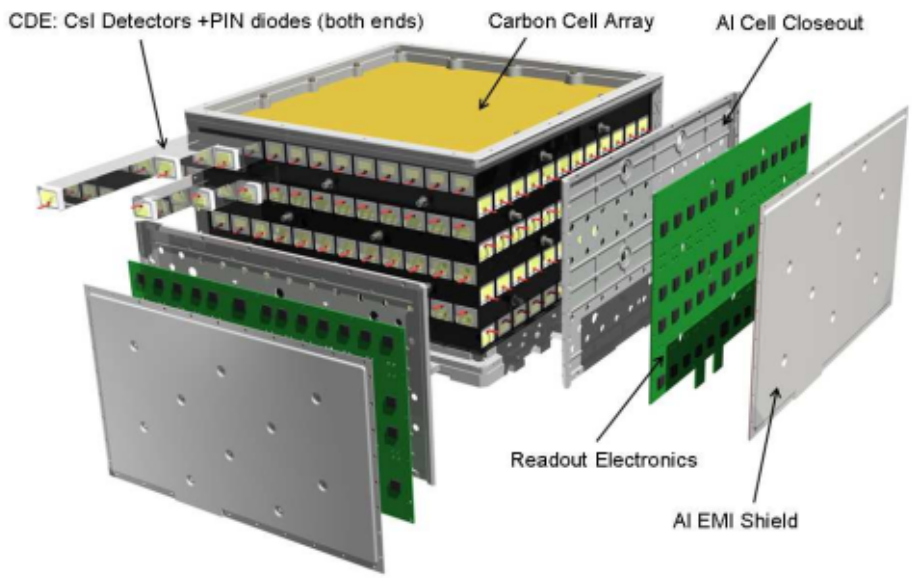

Figure 2.4: The calorimeter module of LAT[4].

Figure 2.4 shows the calorimeter module of the LAT. The calorimeter quantifies the energy of gamma rays due to the shower from e^+ and e^- produced. It also provides the profile of the development of the shower, which helps us in background discrimination[[4],[25]]. It consists of layers of cesium iodide (CsI) crystals. Upon the entry of a γ-ray (or the resultant pair) into the calorimeter, it imparts energy in the form of scintillation light. The quantity of light generated is directly proportional to the energy of the gamma ray, facilitating accurate energy measurement[4].

2.2.4 Data Acquisition System (DAQ)

The DAQ is tasked with the collection, processing, and transmission of data from the tracker, calorimeter, and ACD to the ground. It encompasses electronics for signal triggering, digitization, and information flow management[4]. The DAQ system guarantees effective data management and reduces data loss during transmission.

2.2.5 Interaction process

The LAT interaction mechanism encompasses pair-production processes, when a γ photon interacts with the nucleus, leading to the formation of an electron-positron pair. The incident photon must possess energy exceeding 1.022 MeV. To incorporate pair production in LAT, a converter-tracker is used. The converter-trackers are 16 planes of high-Z materials that provide the interaction cross-section for the pair-production process[4, 23]. The choice of high-Z materials is made because the interaction cross-section for the pair production process for the given energy range is higher for such a type of material. The position-sensitive detectors for the tracking are placed in the interleaved spacing of the converter planes for tracking the charged particles generated via pair production.

Chapter 3

Methodology

This chapter describes the methodology used for the development of the simulation model. The initial phase of our methodology focuses on the construction of the simulation model with the help of the GEANT4 toolkit.

3.1 GEANT4 toolkit (Geometry and tracking)

It is a toolkit developed by CERN for simulating the interaction of particles with materials. It incorporates a wide range of functionalities, like particle tracking, geometry, physics models, and hits collection[21]. The available physics processes incorporate a broad spectrum, including electromagnetic, hadronic, and optical processes, etc. [26]. It incorporates an extensive energy range beginning above a few keV and reaching into the PeV range. It has been designed and built to reveal the utilized physics models, accommodate complicated geometries, and facilitate its seamless adaptability for optimal application across many contexts, like Space, medical, nuclear, etc.

It was developed with software engineering and object-oriented technologies, implemented in the C++ programming language[27, 21]. It plays a crucial role in diverse domains, including high-energy physics, space science, and nuclear physics, where precise and comprehensive models of particle interactions are crucial.

3.2 Proposed routine for the model development

The GEANT4 framework is based on Monte-Carlo simulations[21, 7, 27]. In this framework, we mainly tell the GEANT4 kernel about two things: (i) Experimental Scenario. (ii) Transport scenario of the particle.

Experimental Scenario: Here we describe the geometry, materials, particle properties, sensitive elements, etc. [28, 29].

Transport scenario of particles: Here, the description about the Physics models, Tracking, and storing information is to be provided[28].

A proposed process for model generation utilizing Geant-4 is summarized in Figure 3.1.

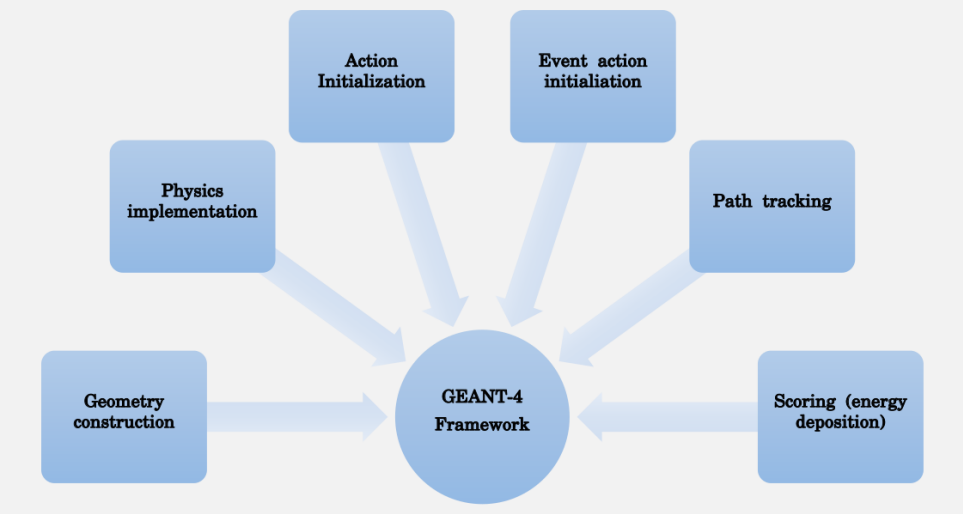

Figure 3.1: The GEANT4 Framework

The forthcoming sections elucidate every stage of the above routine.

3.2.1 Geometry Construction

This allows us to specify the geometry, materials, sensitive elements, and fields like $\vec{E}$ and $\vec{B}$ present in the detector. Geant4 allows three conceptual layers of geometric volumes to define any geometry. They are as follows:

- **Solid Volume -** This describes the shape and size of the volume. E.g., Box, cube, cylinder, tubs, etc.
- **Logical Volume -** It defines the material that has to be filled in the solid volume. Also, we can define volumes that are to be placed inside the solid volume, known as the daughter volume, for the given mother volume. It also defines volume for the detector part, which will collect the hits of particles and store energy or other information. This part of the detector is known as the Sensitive element, and the volume associated with the detector part is known as the Sensitive volume.
- **Physical Volume -** This is analog of real detector system. It will place different parts of the detector in all volumes without letting them overlap with each other.

3.2.2 Physics Implementation

The physics employed for defining a particular process that has to be implemented in the detector for studying the well-defined interaction of the particle with matter, which determines the outcomes of the interaction. We employ various physics models to simulate electromagnetic, hadronic, [30, 31] and optical events at this stage. Geant4 physics covers nearly all particles over energies ranging from 0 to ≈TeV. Users can customize the physics processes and models utilized in their simulations by creating physics lists[21, 29]. To define any of the customized physics lists, we need to implement an important interface method:

1. The Construct Particle interface method defines a list of particles to be used in the application.

2. The Construct Process interface method defines a list of physics processes for the interaction of particles with the matter for a given particle type.

3. The Set cuts interface method defines cuts for the production thresholds.

Geant4 also provides an in-built physics list which can be used according to the needs. Methods for mitigating bias and variance to enhance the effectiveness of simulations, particularly in the context of rare event identification.

3.2.3 Action Initialization

At this stage, we describe primary and secondary particles and their properties, such as energy, momentum, and direction, in the **PrimaryGenerator**[21, 29]. The primary particle means the particle that started the events. These primary particles are tracked in the geometry with physics interactions and generate secondaries, detector responses, and scores. We can use particles as point-like or in the form of a distribution function like Gaussian, etc.. Subsequently, we implemented loops for each generated event to track the particles and initialize them.

3.2.4 Event Action

At this stage, we create an events variable that manages the generation, processing, and storage of simulated events. After that, we put a loop on every event for **runaction**, which regulates the implementation of several events, enabling users to gather and assess data over multiple iterations[26]. The event variables are stored in the form of ntuples, and these variables store information related to the physical quantity for the detector system. For better understanding, we can define histograms and other plots here for the variables.

3.2.5 Tracking & Scoring

This is the heart of any detector simulation. At this stage, we track particles and store information about the variables created in the event action, such as position, energy deposition, etc. Tracks (particles with kinematic information) are put in a stack. To get the information, these tracks are called, and they will pop out for the complete analysis. And the Scoring class will do the necessary analysis, and the information will be stored. The pop-up track is killed to make the memory free. Here, users can create user hook actions on their own to store the information [28].

3.3 Visualization

GEANT4 offers various tools for viewing geometry, particle paths, and detector responses. Interfaces designed for configuring simulations and displaying outcomes, encompassing OpenGL, RayTracer, Qt, etc. [21]. The initialization of the visualization is done via a set of commands in the macro file or via the commands from the user interface. The macro file is a human-readable format containing the necessary commands for the user interface. All the commands given here are with the full path directories.

Chapter 4

Preliminary Configuration of Detector

In this chapter, we describe the results of the simulation of our detector model with GEANT-4. This covers the overall arrangement of geometry, particle types with energy, interaction processes, and the sensitive elements of the setup for tracking particle hit coordinates and energy deposition analysis.

4.1 Geometry Description

For the geometry construction, we created a world volume with dimensions of $40cm * 40cm * 20cm$. A world volume in GEANT4 is the volume beyond which no physical interaction is possible. The world volume is filled with Air, formed by combining elements like C, N, and O. For the material creation, we need to specify the elements with their atomic numbers, symbols, and names, the number of components of these elements present in the material, and their density specification. For our case, the created material density is specified as 0.00120479 g/cm^3. Figure 4.1 shows the simulation result for the above description.

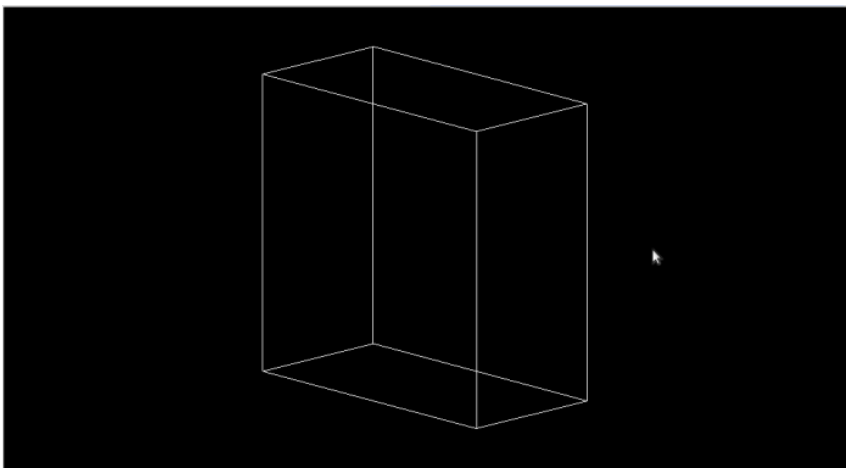

Figure 4.1: The simulated world volume box filled with material as Air.

Further moving to the more realistic system for Anti-Coincidence detector, we created two boxes, the bigger one is the world volume filled with material "Plastic (polyvinyl toulene)" to replicate the plastic scintillators tiles. The density of plastic filled inside the world volume is 1.032 g/cm^3. Inside it, we place a small box in which we place our tracker module. The outer boundary of this box is wrapped with plastic to replicate the plastic scintillators. The inner box is filled with "Air," and we will place our tracker module. Figure 4.2 shows the simulated result for the above description:

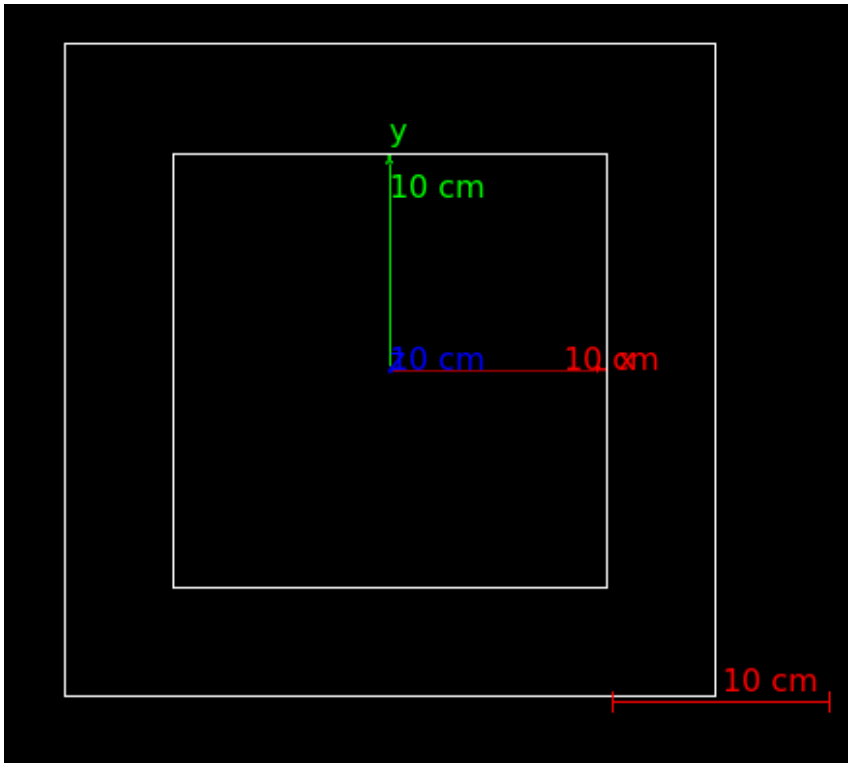

Figure 4.2: The simulated Anti-Coincidence module schematic view without particles.

4.2 Physic Model Implementation

Since we are focusing on Space-Based detectors, we will implement the process of Pair production in our simulation model because in the GeV range of energy, it is the most dominant process. This can be done in GEANT4 by using a predefined physics list or by creating used user-defined physics list.

The predefined physics list contains a series of processes, and if you incorporate it into your simulation, then all processes will be implemented in the simulation. Thus, it's better to implement the user-defined physics list. We use user user-defined physics list to incorporate pair production in our simulation.

4.3 Particle creation with its properties

For creating particles, we can use the "findparticle" module of GEANT4. Here we can find the predefined particles in GEANT4, or we need to create a particle in the physics list module. For our simulation model, we created a gamma particle and incorporated it first into the geometry shown in Figure 4.1 for testing purposes. The Gamma particle created has the energy of 50 GeV, and the momentum direction is along the Z-direction.

Particle gun: The point where this particle will be bombarded anywhere in the geometry is known as a particle gun, and for this case, it is placed at the center of the geometry.

After this, we need to initiate all actions for running the simulation using the "Action Initialization" module. Figure 4.3 shows the simulation result for the above description.

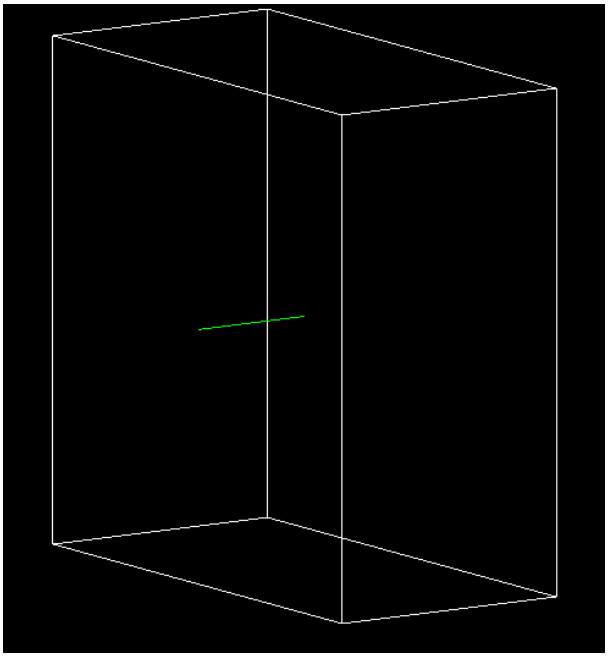

Figure 4.3: The simulated geometry with created gamma particle having energy 50 GeV.

After initiating the actions, we will be able to generate the track object, which will be used to identify the tracking objects. These tracking objects store two types of information associated with the tracked particles: (i) Static Information. (ii) Dynamic Information.

The static information contains information about the mass and charge of the particles. The dynamic information contains information like position, time, energy, momentum, polarization, etc. The information of polarization will be stored when there will be $\vec{E}$ or $\vec{B}$ is incorporated in your detector geometry.

4.4 Tracker Module

Figure 4.4 shows the tracker module simulations for which we have chosen "Silicon" as material and created silicon stipes, each having dimension $50cm * 1cm * 1cm$ and they are arranged in the same layer, having a gap of $1mm$ between two stipes in the same layer. The next layers are placed in a crossed manner to this layer just above it, and similarly, this pattern repeats up to 11 layers. The crossed arrangement of stripes gives us better resolution for the detector.

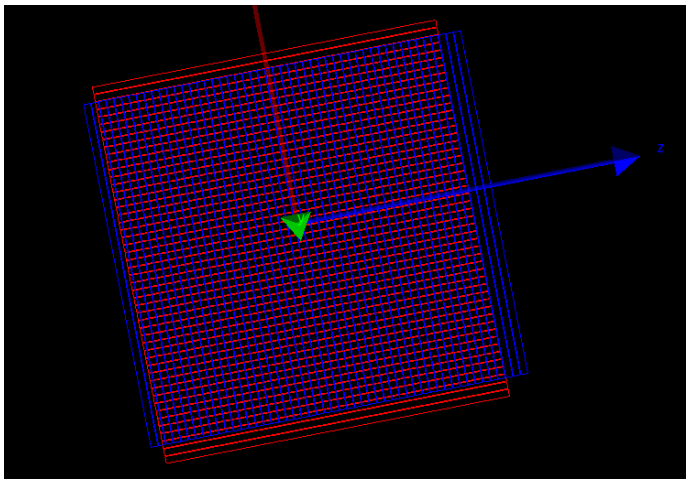

Figure 4.4: Top view of tracker module.

Figure 4.5 (a) shows the final configuration of the detector module integrated with the Anti-coincidence module with tracker and gamma particle falling on each site.

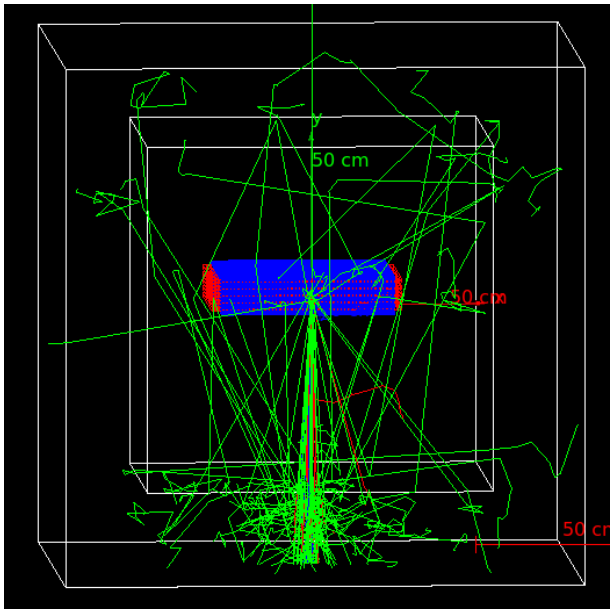

Figure 4.5: The simulated ACD and tracker Module integrated. A gamma particle of 100 GeV is hitg on it.

The larger box contains "Plastic"(Anti-coincidence film) and acts as an Anti-coincidence module. The smaller box has a sensitive tracker module to track particles and calculate energy deposits. The smaller box is filled with "Air". The tracker module placed inside the smaller box is a sensitive element that will record the hits and energy deposited on it.

Figure 4.6 shows the top view of the detector. The incoming particle is a "Gamma photon" of energy "100 GeV"(Green line = tracks of photon) and having direction toward the $-y$ axis.

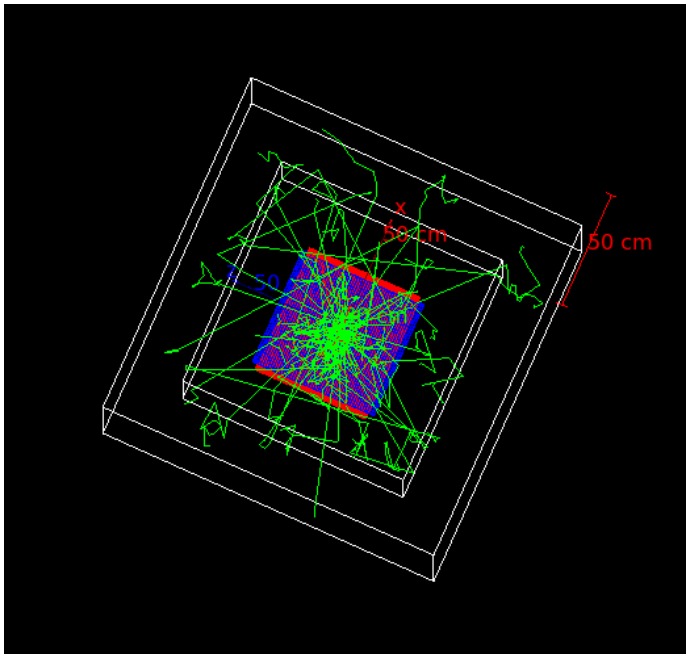

Figure 4.6: Top view of particle hitting the detector.

Physics Interaction: Here Pair-Production is implemented with Bremsturlung process.

Copy Number: Every particle detecting site of the tracker module is uniquely identified with a particular positive integer number known as the copy number.

After the initial development of the simulation model, we have done some preliminary analysis for the model, which has been summarized in the forthcoming section on analysis.

4.5 Analysis

In this section, we present some of the preliminary results for the simulation model. Figure 4.7 shows the variation of No. Of entries v/s the copy numbers for the complete shower. From this, we conclude that the top layer (Higher copy number) has fewer entries because the shower has started, and as we go towards the middle layers, entries increase because we have more e^--e^+

pairs which undergo the Bremstrahlung process and further initiate the shower, and at last, the entries diminish as it goes out from the tracker module, so no tracking can be done.

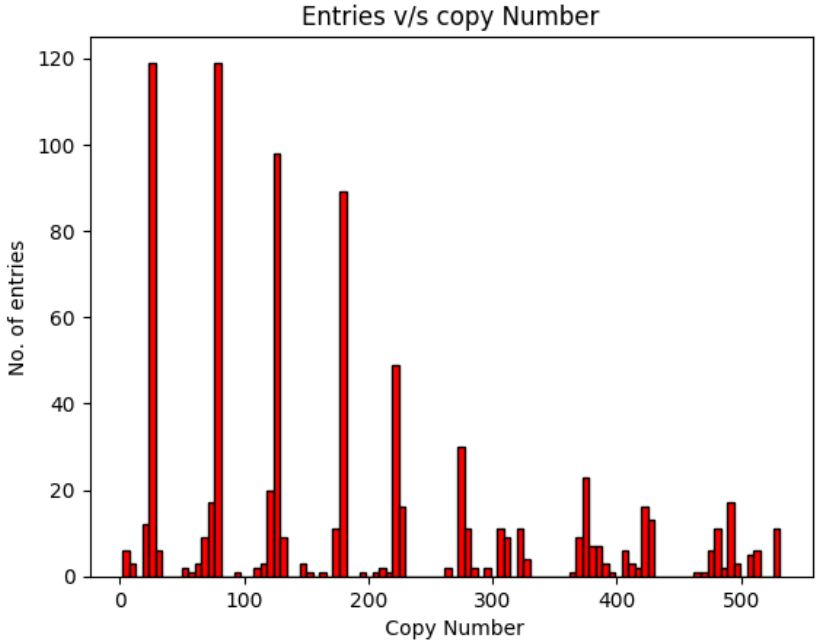

Figure 4.7: Variation of No. of entries w.r.t Copy number on the tracker module sites.

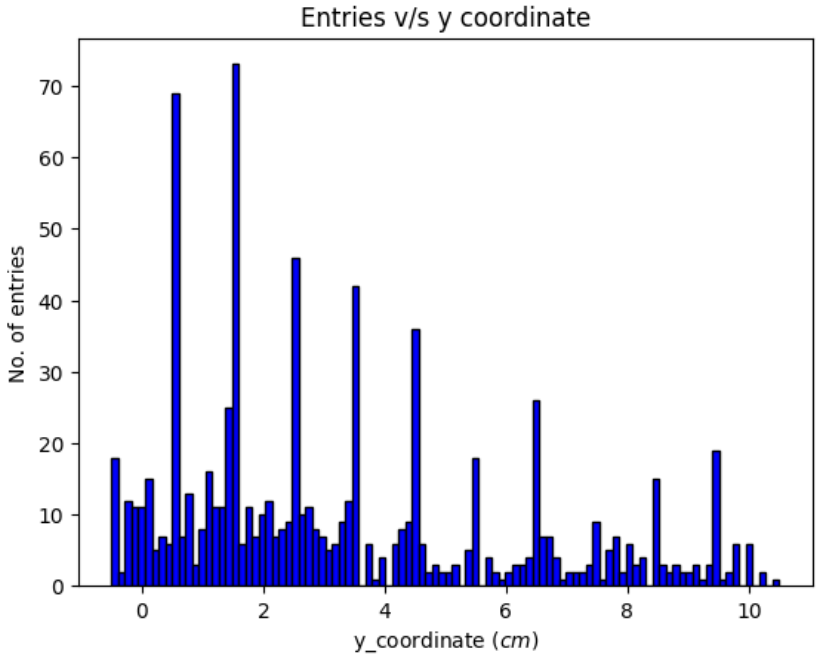

Figure 4.8: Variation of No. of entries w.r.t Y coordinate of particle hits. This is important because our tracking strips are arranged in a stack form along the Y-direction.

Figure 4.8 shows the variation of No. Of entries v/s change in Y-coordinate for the entries of the complete shower. As the topmost layer has high Y coordinate values and there the shower has just started, thus we have less no. of entries and it is shown in the figure. As we move toward the middle layers, the entries will increase, which is shown in the figure for the Y coordinate below $6cm$. We have some entries after $y = o$, this is because our last layer is at $y = 0$, i.e, $x - z$ plane, and we have a finite thickness of $1cm$ for each stripe. So we can have some entries below y=0. After that, we do not have any tracking elements, so we cannot further propagate any particles.

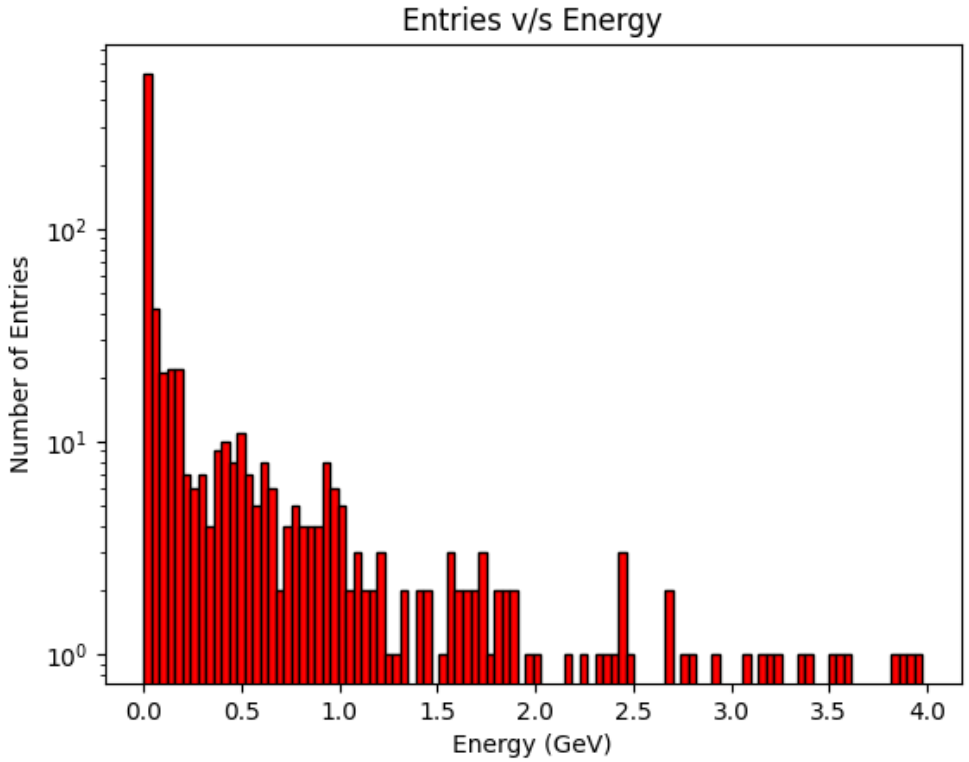

Figure 4.9: Variation of No. of Entries v/s Energy Deposit at the particular particle sites in the tracking module.

Figure 4.9 shows the variation of No. Of entries v/s Energy deposited for the complete shower. From this, we can conclude that a very small fraction of energy is deposited on our collecting stripes, as the thickness of our silicon stripes is 1 cm. Thus, we understand that if we increase our detection volume, we can collect more energy. Also, the higher value of energy is deposited at the topmost layer sites, and very few entries are there in the top layer.

Chapter 5

The Fermi LAT configuration simulation: Realistic description

In this chapter, we describe the results of the simulation of our detector model, similar to the Fermi LAT configuration with GEANT-4. This covers the overall arrangement of geometry, particle types with energy, interaction processes, and the sensitive elements of the setup for tracking particle hit coordinates and energy deposition analysis.

5.1 Geometry Simulation

This system assesses a payload containing two detector modules: (i) Anti-coincidence module and (ii) Tracker (TKR) module.

5.1.1 Tracker module

For the tracker module simulation, we choose Si tracker planes, each having thickness of 400 μm along the z-direction, with $4 * 4$ Si single sided silicon detectors in each Si Plane in square tile form, each having dimension of 9 cm $*$ 9 cm along X and Y direction and thickness same as 400 μm. Every consecutive single-sided square tile in a particular Si Plane is separated by a distance of 200 μm. The complete dimension for each Si plane is 36.06 cm $*$ 36.06 cm along X and Y directions. The density of Si material for the simulation is 2.333 g/cm^3.

Figure 5.1 shows a single simulated Si plane tile with thickness 400 μm and Figure 5.2 shows the simulated single-sided Si detector in each Si plane tile of the tracker module layer for the $4 * 4$ single-sided configuration.

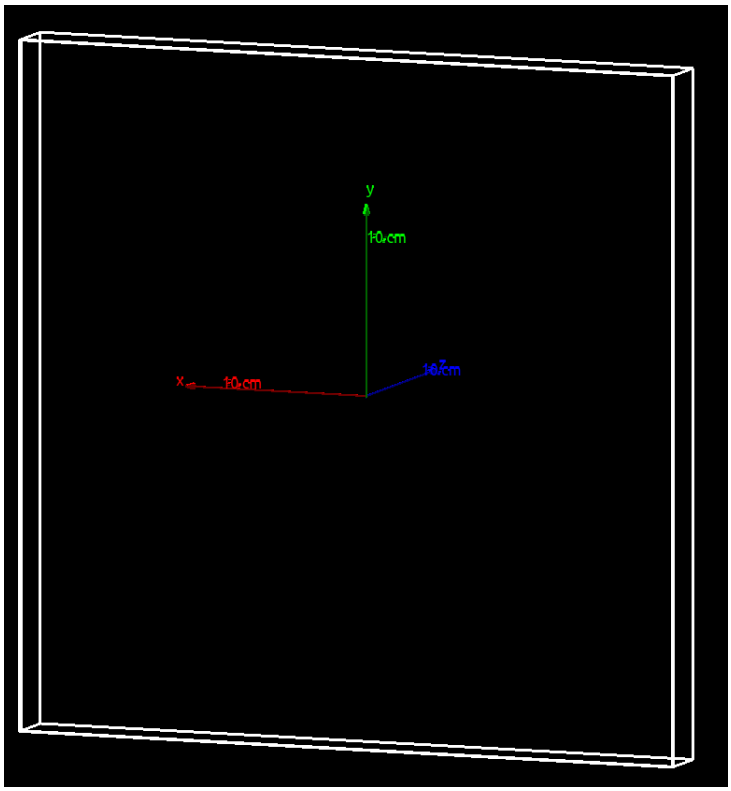

Figure 5.1: The simulated Si tracker plane of the tracker module.

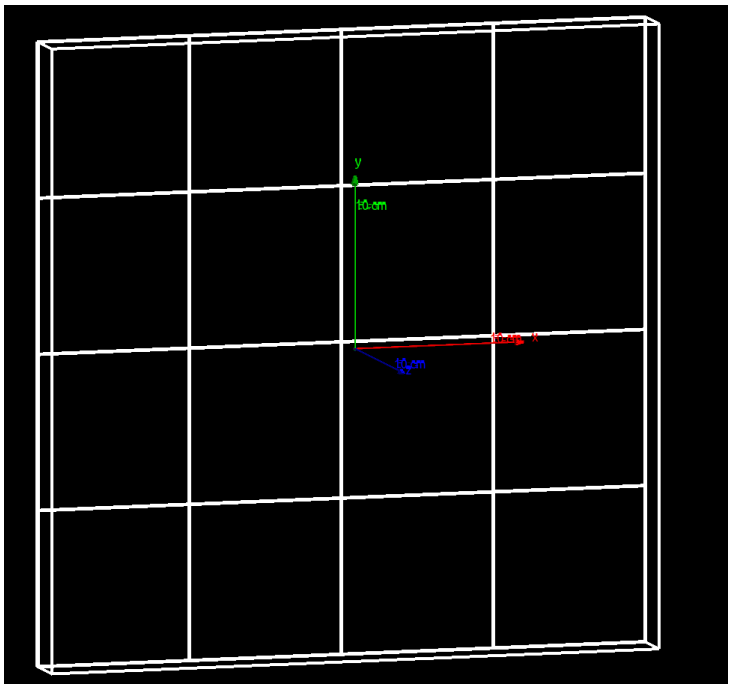

Figure 5.2: A simulated Si tracker plane with single side Si detector for $4 * 4$ configuration for the tracker module.

Every consecutive tracker layers of Si tracker planes (XY plane) are interleaved with tungsten converter foil of density 19.3 g/cm^3 and thickness of 300 μm. The converter foil is arranged just above the tracker plane and will be parallel to the tracker plane, and this pattern has to be repeated for the complete tracker configuration. The distance between the Si plane and the consecutive converter foil is 1 mm. Figure 5.3 shows the simulated converter foil (Solid plane) in red colour with the Si tracker plane layer next to it (white plane).

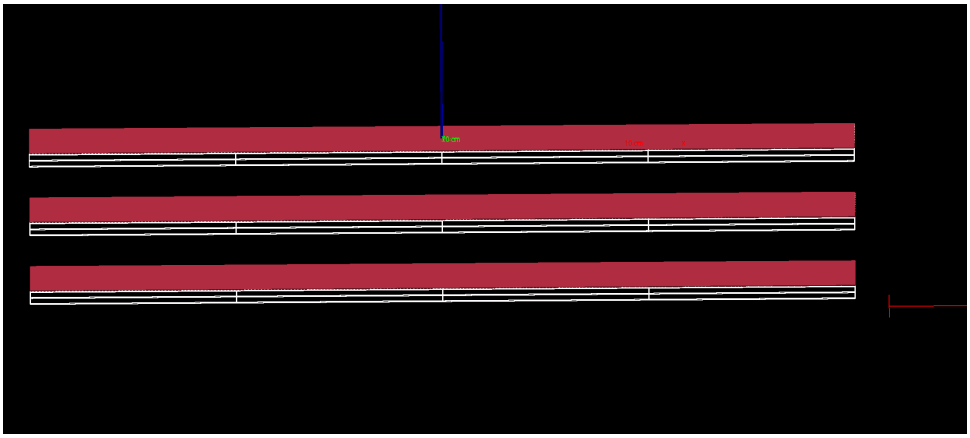

Figure 5.3: The simulated converter foil of high-Z material between the two consecutive Si tracker planes. The separation between foil and tracker is 1mm.

Each of the consecutive Si plane of tracker modules are separated by a distance of 3 cm from each other.

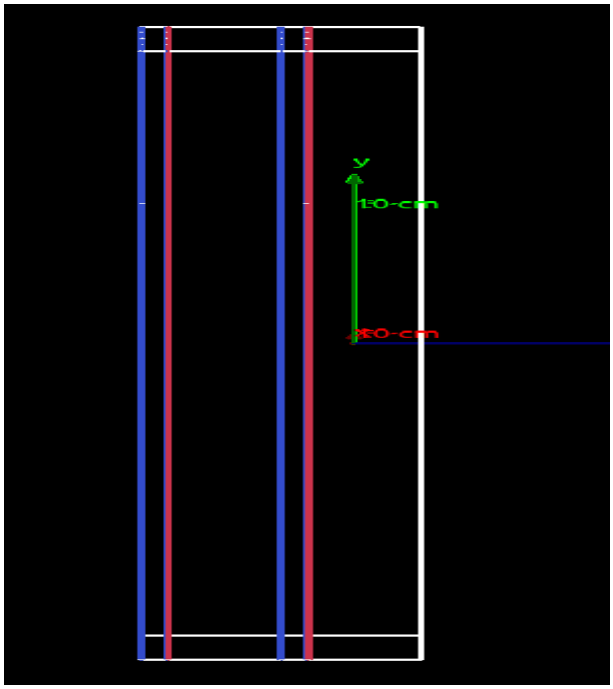

Figure 5.4: The Active Tile of Si plane with converter foil and mechanical support. The mechanical support gives stability to the tracker and converter plane.

Figure 5.4 shows the simulation arrangement of the Active part of the tracker plane (blue Colour) and converter foil (red colour), supported by a mechanical thickness support to give stability to the tracker planes. The Si Plane also has a non-sensitive border of the width of 1.5 mm around it, which acts as a dead region for the Si Tiles.

Each layer of single-sided square tiles in each Si plane has 2 viewing modes, which are further subdivided into ladders and stripes, so that they are arranged in orthogonal planes and they act as the active region of the Si tile for charge particle detection. Figure 5.5 shows the simulated configuration of the Active tracker stripes module:

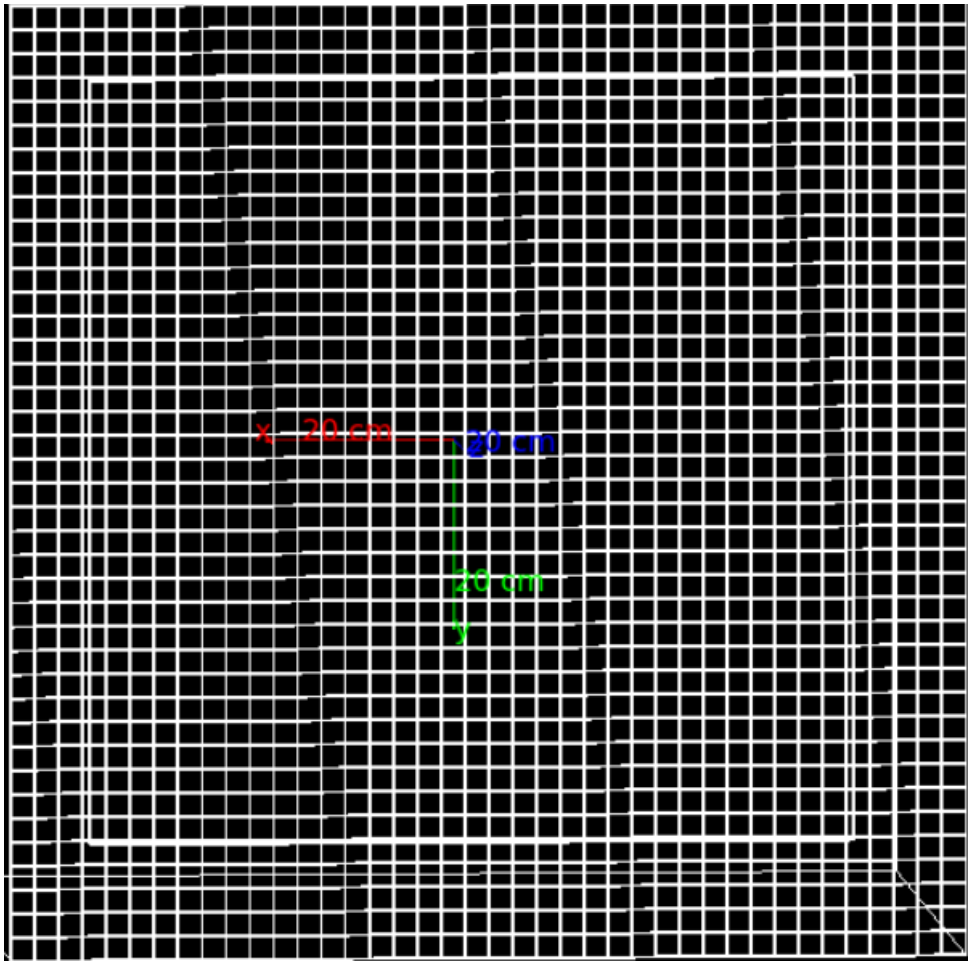

Figure 5.5: The tracking stripe in each single-sided Si tile is arranged in an orthogonal fashion to each other.

Combining all tracker planes, with converter foil and active detector tile (ladder and strip) for orthogonal plane, we get the complete tracker module, which has 15 Si tracking layers and 12 converter foil planes (except for the 1 and last plane). Figures 5.6 and 5.7 show the complete simulation of the tracker module for the detector:

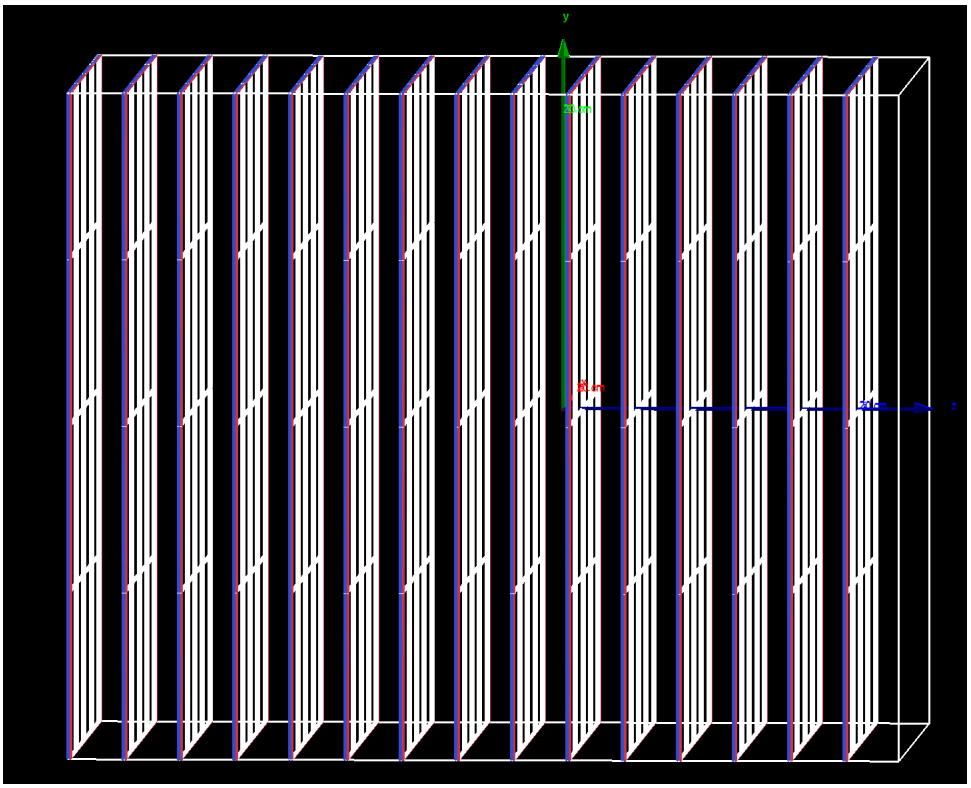

Figure 5.6: The complete tracker module of the detector: sideways view

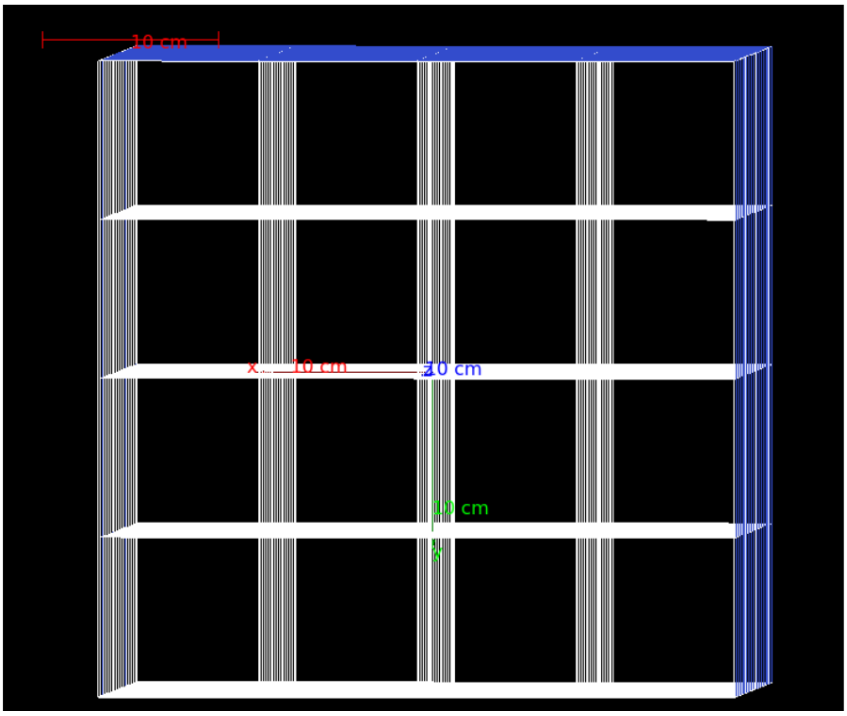

Figure 5.7: The complete tracker module with 4*4 single-sided tracker of the detector: front/top view

5.1.2 Anti-coincidence detector (ACD)

For the ACD geometry, we have two different tile configurations; one in rectangular shape for the sideways portion (lateral configuration) and the other in a square shape for the front and back portions. The dimension for a square tile is $40.6cm * 40.6cm * 1cm$. The tile is filled with scintillating material like "Plastic(polyvinyl toulene)" to replicate the plastic scintillators tiles. The density of plastic filled inside is 1.032 g/cm^3. The dimension of the lateral tile is $50.5cm * 40.6cm * 1cm$ and the square and rectangular tiles are arranged 90 degrees from each other with a small gap of 100 μm. Figure 5.8 shows the simulated tiles for the sidewall portion and the top/front portion (seen from the left side of the image) of the ACD.

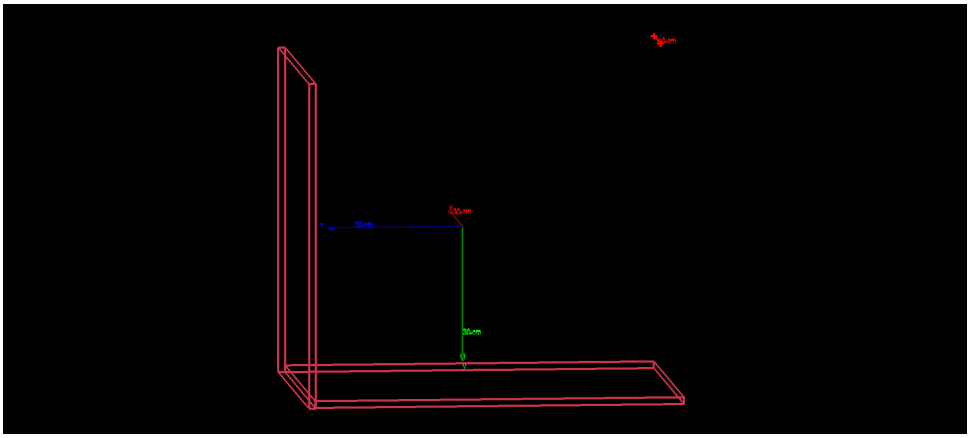

Figure 5.8: The lateral and the front tiles of the ACD module. Front tile: The Tile (left side of the image) and the lateral side are seen at the bottom.

This back tile will be the replica of the front tile (square shape), and the rest tiles are the replica of the lateral tile, and all together will complete the configuration of the ACD with all 6 faces and each tile filled with the plastic scintillator material. Figure 5.9, shown below, is the simulated result for the complete ACD module of the detector.

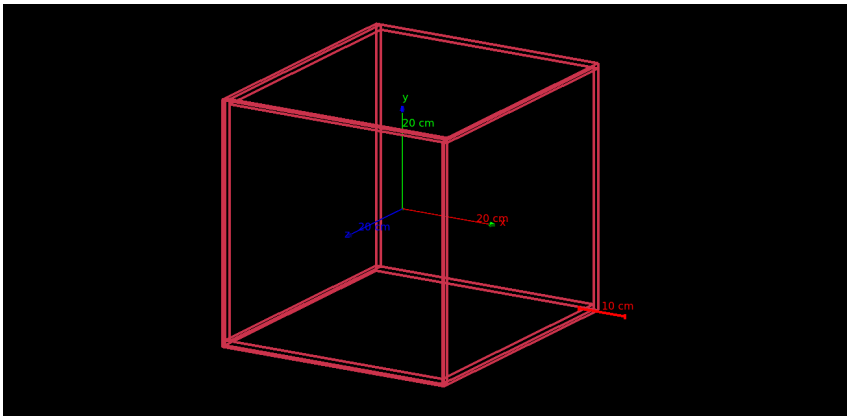

Figure 5.9: The Anti-coincidence Module of the simulated detector:

5.2 Physics Module implementation

Since we are focusing on Space-Based detectors, we will implement the process of Pair production in our simulation model because in the GeV range of energy, it is the most dominant process. This can be done in GEANT4 by using a predefined physics list, which also contains a series of processes, and if incorporated in the simulation, then all processes will be implemented in the simulation. For this simulation configuration, we are using a predefined physics list, the electromagnetic physics option 4, FTFP BERT (for gamma particle process), and the decay physics. These physics lists incorporate processes like pair-production, Compton scattering, bremsstrahlung, multiple scattering, and photoelectric effect in Geant4 and many more for different energy ranges of the particle.

5.3 Particle creation: Specifying particle properties

The creation of particles for this simulation is done using the "findparticle" module of Geant4. The particle used here is a point-like gamma particle, having an energy of 1 GeV, and it is coming toward the detector system in the form of a cone with an opening angle of the cone of 10 degrees. The other properties of these gamma particles are already defined in the built-in module.

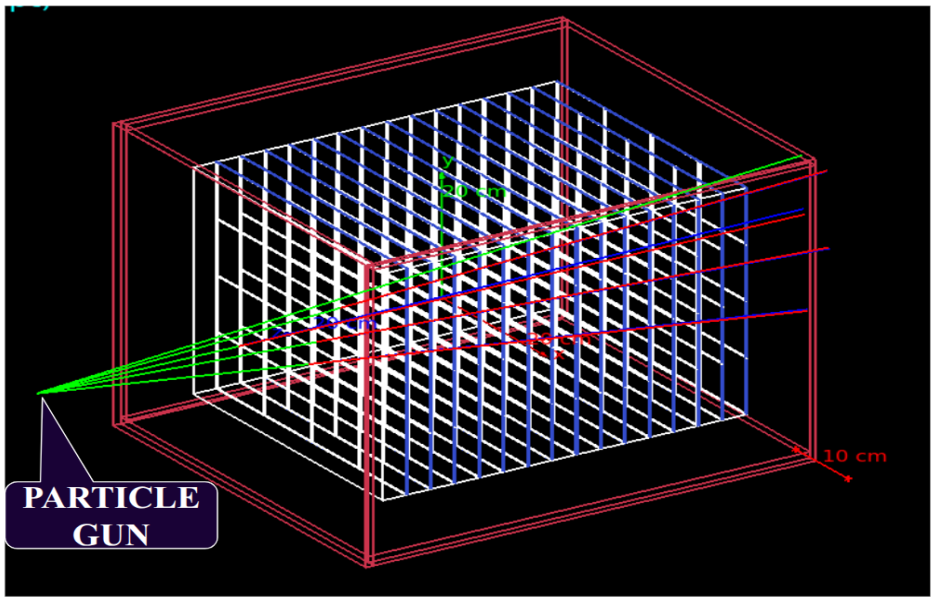

Figure 5.10: The simulated Anti-coincidence Module integrated with the tracker module for the detector for pair production process only. The incoming particles are gamma of energy 1 GeV (green) split to red (e^-) and blue (e^+). The number of particles per event is 1, and a total of 5 events are simulated.

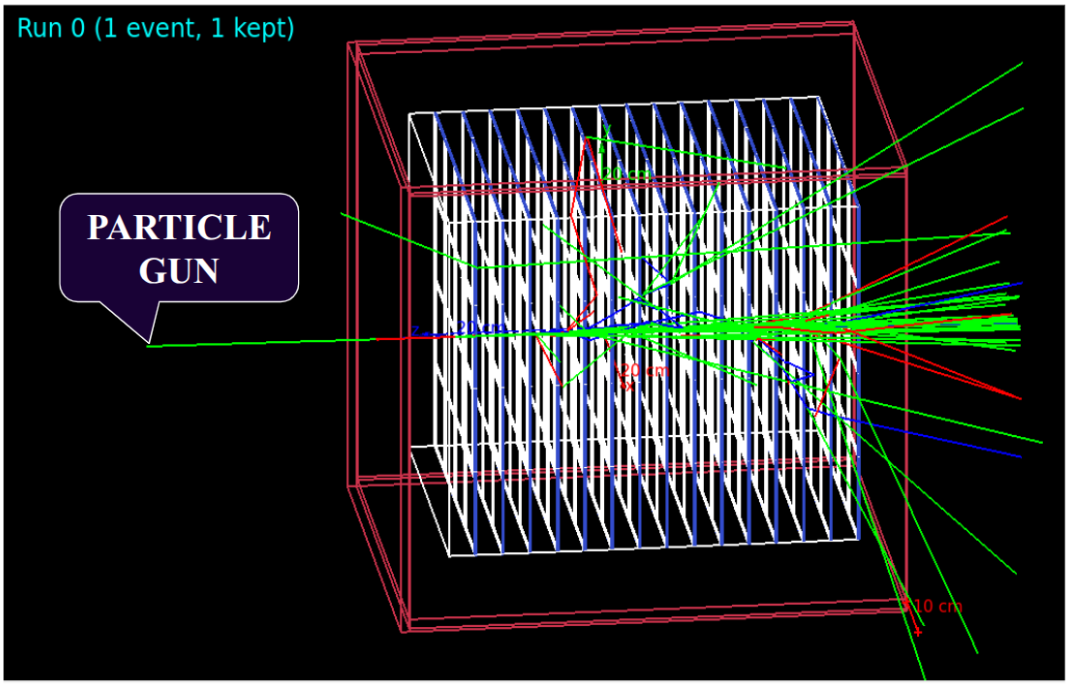

Figure 5.11: The simulated ACD integrated with tracker implementing all major processes from the in-built physics list for the gamma particle for the detector module.

Figure 5.10 shows the simulation of an integrated module of ACD with a tracker system only for the pair-production process with 5 gamma particles, each of 1 GeV energy, falling on it in the form of a cone at an opening angle of 10 degrees.

Similarly, Figure 5.11 shows the simulation for all processes from the in-built physics list for a single gamma particle per event of energy 1 GeV, falling in the form of a cone having a cone opening angle of $10°$.

5.4 Analysis for the Detector Configuration

In this section, we present some of the analysis results for this particular geometry of the simulation model.

5.4.1 For the particle of 1 GeV energy and given converter foil thickness.

For this case, we choose converter foil thickness as 300 μm. Figure 5.12 shows the variation of the hit coordinates for a single particle simulation in which the incoming particle has energy 1 GeV and it is coming from +Z-direction and going towards -Z-direction in the form of a cone at an opening angle of $10°$.

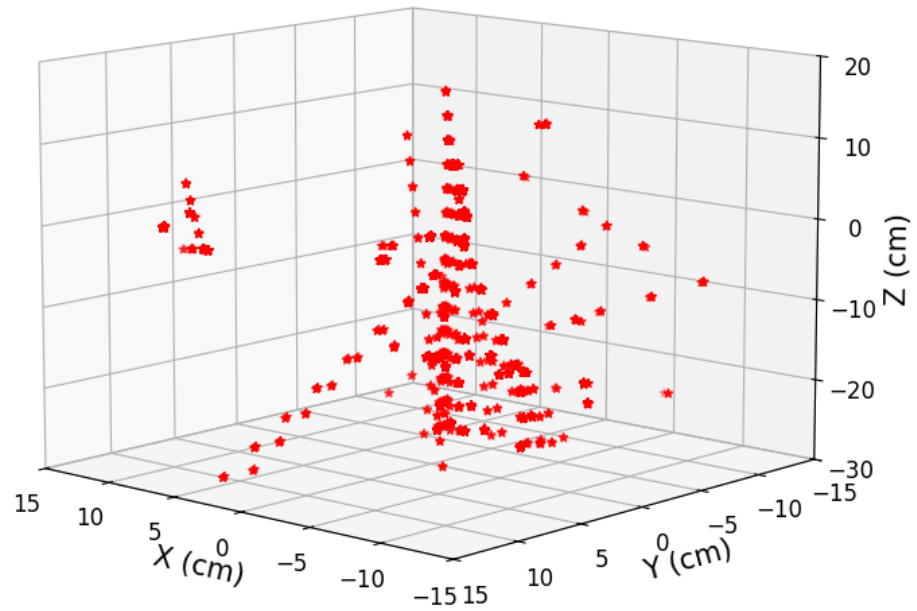

Figure 5.12: Plot of variation of particle hits coordinate. The particle's incoming direction is from +Z-direction in cone form toward -Z with a cone opening angle of $10°$.

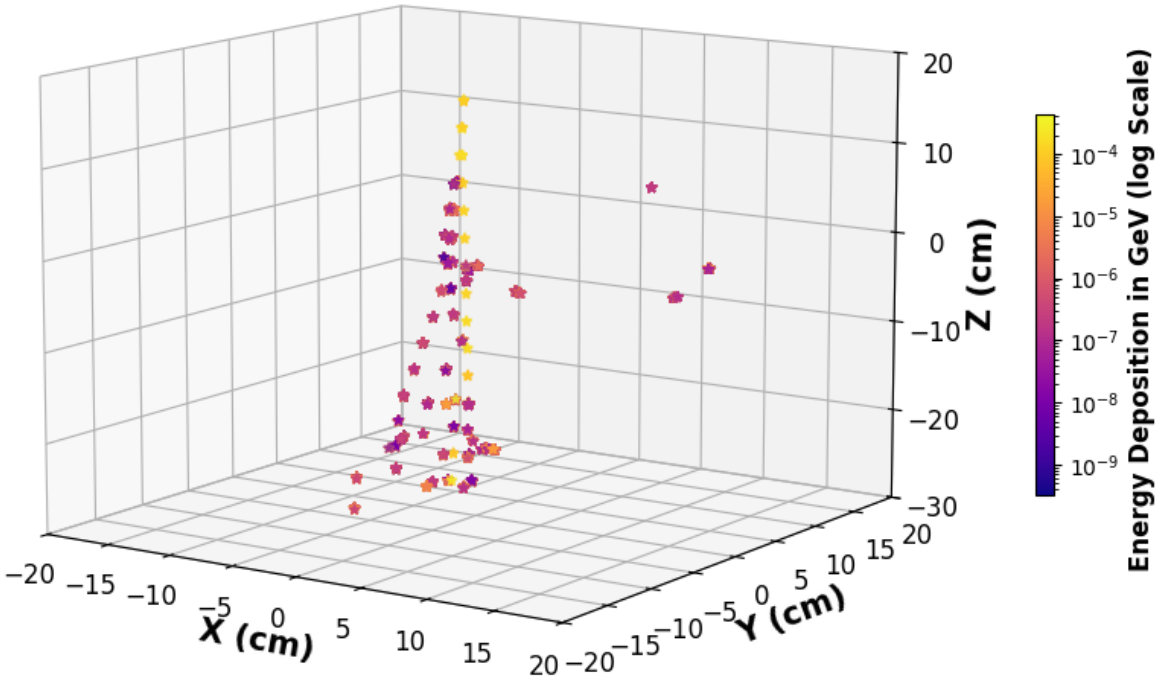

Figure 5.13: Plot of variation of non-zero energy deposition w.r.t hits coordinate for $300\mu m$ converter foil thickness.

Figure 5.13 shows the variation of non-zero energy deposit from the particle hits w.r.t their coordinates. The color bar shows the energy deposited in GeV at a particular hit point.

From this, we can conclude that most particles deposit a very small fraction of energy w.r.t the incoming particle because we have a very small collection area on the tracker sites, because the thickness for the tracker plane is 400 μm. Here, the energy deposition happens due to all processes implemented via the built-in physics list for the simulation.

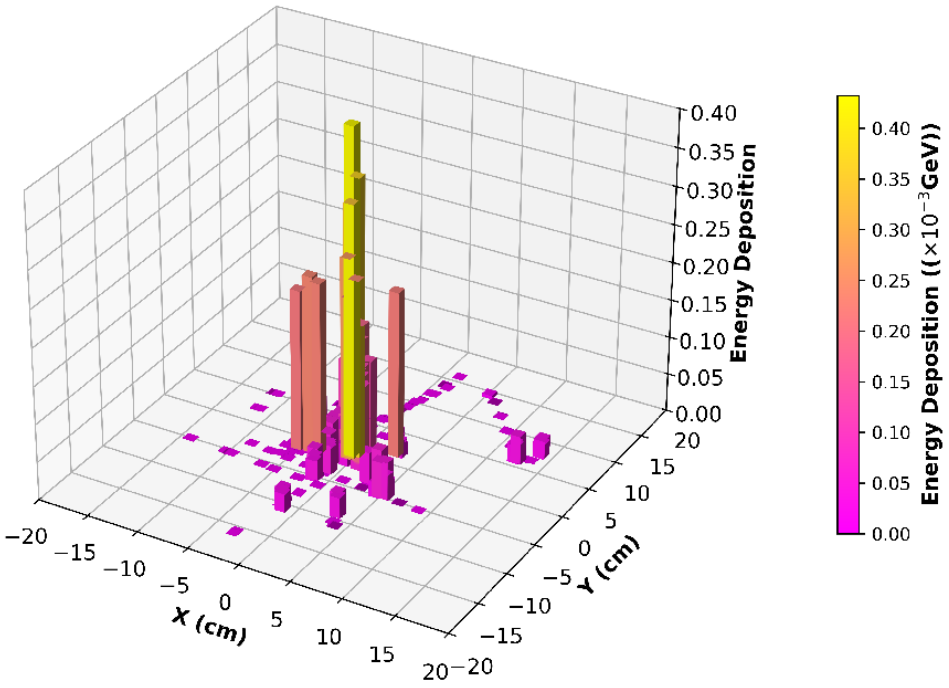

Figure 5.14: Plot of variation of energy deposition w.r.t XY direction of hits for 300μm converter foil thickness.

Figure 5.14 shows the plot for energy deposition w.r.t the XY direction of hits for 300μm converter foil thickness. We are interested in this because, for our simulation, the tracker plane is parallel to the XY plane.

5.4.2 Effect of thickness of converter foil on the detector module.

For this case, we have doubled the thickness of the converter foil to 600μm, keeping the particle energy, material for the converter foil, the dimensions for the Si tracking planes and active region, the same as the previous case. Figure 5.15 shows the variation of the hit coordinates of the particle for the simulation where the incoming direction of the particle is from the +Z-direction and it will go toward the -Z-direction in the form of a cone at a cone opening angle of 10°.

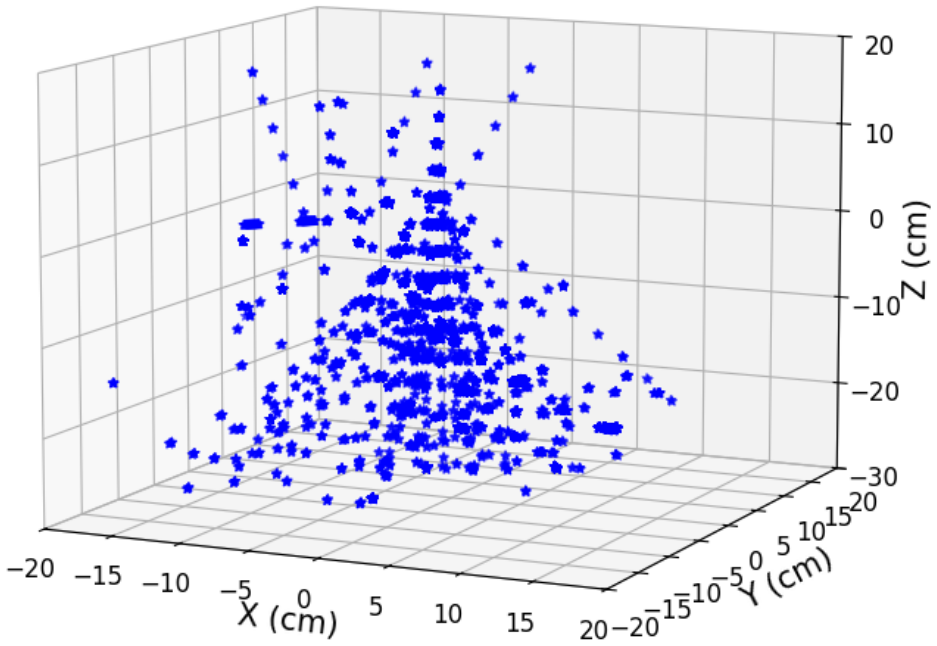

Figure 5.15: Plot of Position hits of the particle for double converter thickness.

From this plot, we conclude that if we double the converter thickness, the number of entries increases because we have more interaction available for the incoming particle for the pair production and other processes from the physics List.

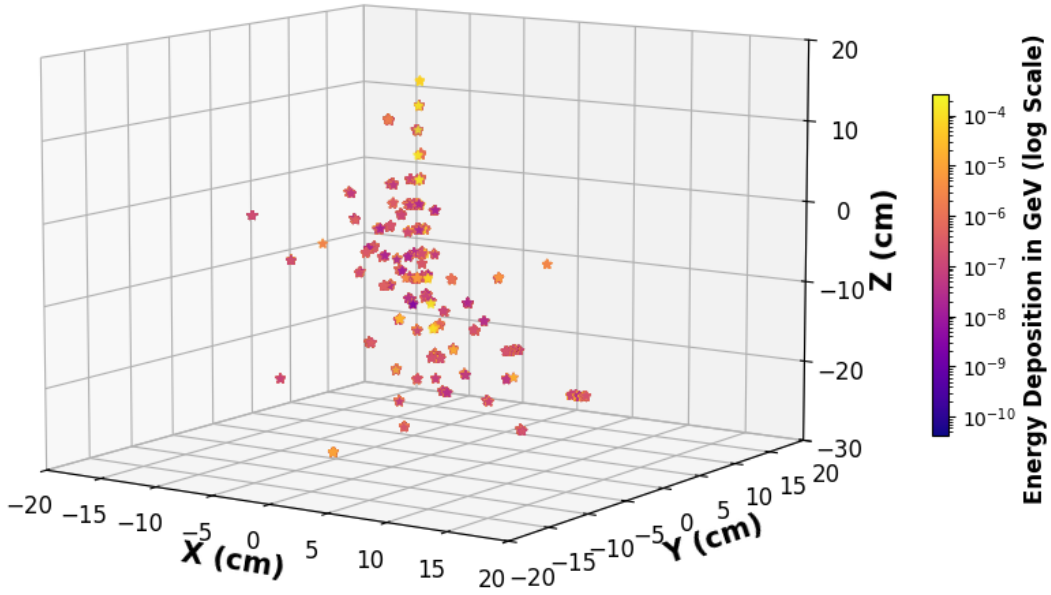

Figure 5.16: Plot of variation of non-zero energy deposition w.r.t the hit's coordinate for double converter thickness.

Figure 5.16 shows the variation of non-zero energy deposit from the particle hits w.r.t their coordinates for doubling the converter foil. The color bar shows the energy deposited in GeV at a particular hit point.

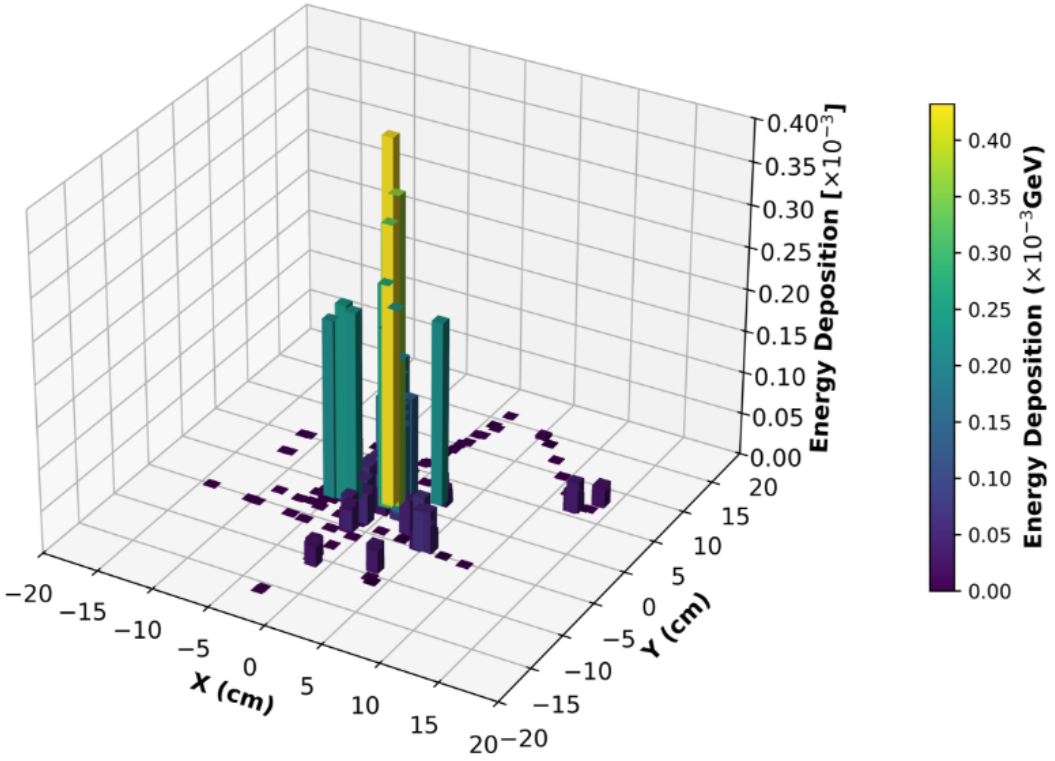

Figure 5.17: Plot of variation of energy deposition w.r.t XY direction of hits for 600 μm converter foil thickness.

Figure 5.17 shows the variation of energy deposition by the hits with respect to the hits of the particle lying in the XY plane direction. We are interested in this because, for our simulation, the tracker plane is parallel to the XY plane.

From both figures 5.16 and 5.17, the energy deposition goes as the same for the previous case, as only the number of entries is increasing, but again, the collecting areas are smaller, so the energy deposition fraction will be low in comparison to the original particle energy.

The only difference we observe here is that the number of interactions has increased, thus, we have more numbers of entries depositing the energy in comparison to the previous case, but the fraction of energy deposited by the incoming particle is very small in comparison to its own energy.

Thus, we understand that if we increase our detection collection volume of the particle, we can collect more energy, which is done by the calorimeter for this type of detector.

Chapter 6

Summary and Scope for Future Work

6.1 Summary

In this thesis, we have effectively executed a GEANT-4 simulation of a GeV detector, emphasizing the modeling of its geometry, physics processes, and the precise creation of primary particles. The comprehensive implementation of the detector geometry ensures realistic particle interactions inside the simulation. By integrating physical processes, we successfully simulated the intricate interactions of GeV particles with the detector material, encompassing different interaction processes like Pair production, Bremstrahlung, Compton, multiple scattering, etc., and can record the energy deposition and no. of entries at the detecting sites with a unique identity number.

This study has developed a comprehensive simulation framework for the GeV detector, and these approaches will enhance existing detector design and provide a robust platform for future advancements in GeV detector technology.

6.2 Future Plan

This study has further improved our understanding of detector development for spaceborne applications. Thus, future work includes:

- Modification of the current design to enhance the sophistication of simulations for track reconstruction, particle identification, and background rejection.
- Additionally, we are characterizing the Geiger-mode Avalanche Photodiode (GAPD) to advance the development of the Anti-coincidence detector. Subsequently, we will attempt to acquire the Silicon Stripes detector, and its characterization has to be done to create the tracking module.

6.2.1 Characterization of GAPD.

To characterize the GAPD, our first objective was to find its breakdown voltage. Since GAPDs work in reverse bias configuration so we have to operate beyond their breakdown voltage range. For this, we try to study the response of GAPD for a given voltage by sending a particle of optical range to it. The particle will have fixed intensity, so the no. of photons is fixed and it has been detected via GAPD and gives a response in the form of a pulse height, which corresponds to the voltage generated by the GAPD.

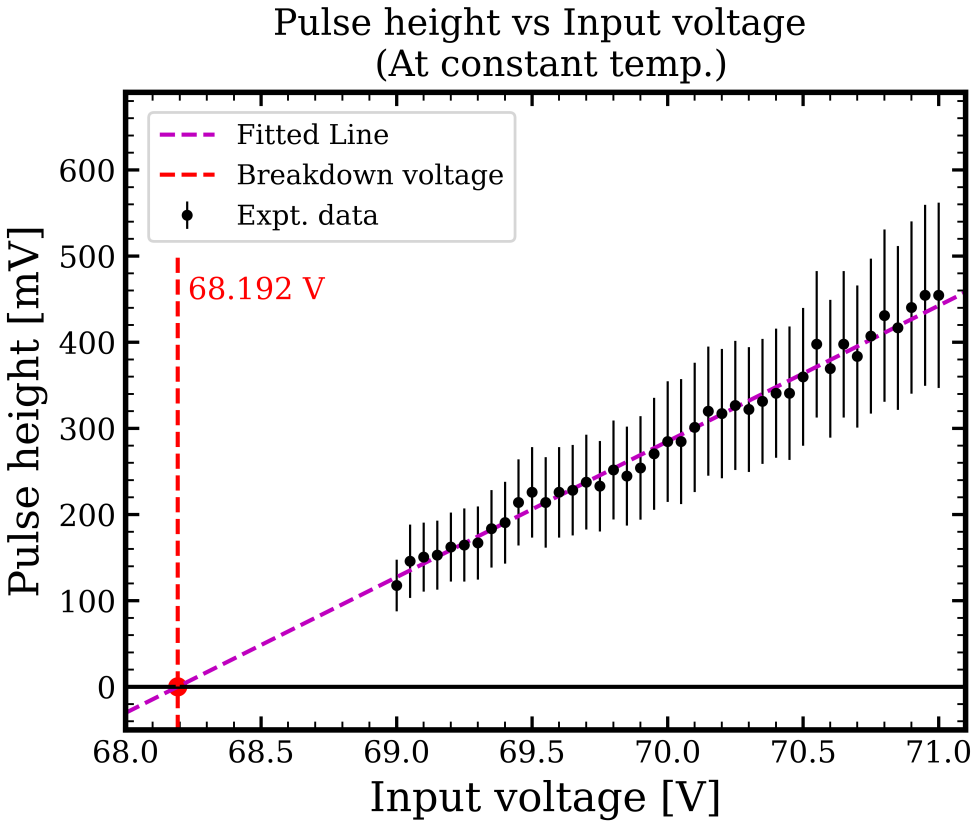

Figure 6.1: Plot showing variation of Pulse height with input voltage supplied to the GAPD. The points correspond to the pulse height in terms of voltage. The point where the pulse height corresponds to zero is the breakdown voltage of GAPD.

Figure shows the variation of pulse height with the input voltage supplied to the GAPD. For the breakdown voltage, we look at the voltage where the pulse height completely vanishes; that point corresponds to the breakdown voltage of the device, which is determined by extrapolating this curve. From this plot, we conclude that the breakdown voltage for the given GAPD detector is 68.192 V.

References

[1] Elisa Prandini, Konstantinos Dialektopoulos, and Jelena Strišković. Gamma rays: propagation and detection. *arXiv preprint arXiv:2211.17021*, 2022.

[2] Ulisses Barres de Almeida. Astroparticle Physics with TeV to PeV Ground-Based Gamma-Ray Detectors. *Braz. J. Phys.*, 55(3):107, 2025.

[3] D. Bose, V. R. Chitnis, P. Majumdar, and B. S. Acharya. Ground-based gamma-ray astronomy: history and development of techniques. *The European Physical Journal Special Topics*, 231(1):3–26, December 2021.

[4] Atwood et. al. The large area telescope on the fermi gamma-ray space telescope mission. *The Astrophysical Journal*, 697(2):1071–1102, May 2009.

[5] Stefan Funk. Ground- and space-based gamma-ray astronomy. *Annual Review of Nuclear and Particle Science*, 65(1):245–277, October 2015.

[6] Bernard Degrange and Gérard Fontaine. Introduction to high-energy gamma-ray astronomy. *Comptes Rendus Physique*, 16(6):587–599, 2015. Gamma-ray astronomy / Astronomie des rayons gamma.

[7] Tullio Basaglia, Zane W. Bell, Daniele D'Agostino, Paul V. Dressendorfer, Simone Giani, Maria Grazia Pia, and Paolo Saracco. Geant4: A game changer in high energy physics and related applicative fields. *Future Generation Computer Systems*, 159:411–422, 2024.

[8] John W. Hewitt and Marianne Lemoine-Goumard. Observations of supernova remnants and pulsar wind nebulae at gamma-ray energies. *Comptes Rendus Physique*, 16(6):674–685, 2015. Gamma-ray astronomy / Astronomie des rayons gamma.

[9] K. Koyama, R. Petre, E. V. Gotthelf, U. Hwang, M. Matsuura, M. Ozaki, and S. S. Holt. Evidence for shock acceleration of high-energy electrons in the supernova remnant SN1006. , 378(6554):255–258, November 1995.

[10] Una Hwang, Anne Decourchelle, Stephen S. Holt, and Robert Petre. Thermal and non-thermal x-ray emission from the forward shock in tycho's supernova remnant. *The Astrophysical Journal*, 581(2):1101, dec 2002.

[11] Bednarek, W. and Bartosik, M. Gamma-rays from the pulsar wind nebulae. *A&A*, 405(2):689–702, 2003.

[12] ENRICO Fermi. On the origin of the cosmic radiation. *Phys. Rev.*, 75:1169–1174, Apr 1949.

[13] Guillaume Dubus. Gamma-ray emission from binaries in context. *Comptes Rendus Physique*, 16(6):661–673, 2015. Gamma-ray astronomy / Astronomie des rayons gamma.

[14] HIROTAKA ITO, MOTOKI KINO, NOZOMU KAWAKATU, and SHOICHI YAMADA. Nonthermal emissions from shocked shells driven by powerful agn jets. *International Journal of Modern Physics D*, 19(06):893–899, June 2010.

[15] Charles Dennison Dermer and Berrie Giebels. Active galactic nuclei at gamma-ray energies. *Comptes Rendus. Physique*, 17(6):594–616, May 2016.

[16] Grzegorz (Greg) Madejski and Marek Sikora. Gamma-Ray Observations of Active Galactic Nuclei. , 54:725–760, September 2016.

[17] Yoshiyuki Inoue. Cosmic gamma-ray background radiation, 2014.

[18] David J. Thompson. Space detectors for gamma rays (100 mev–100 gev): From egret to fermi lat. *Comptes Rendus Physique*, 16(6):600–609, 2015. Gamma-ray astronomy / Astronomie des rayons gamma.

[19] G Sinnis. Air shower detectors in gamma-ray astronomy. *New Journal of Physics*, 11(5):055007, may 2009.

[20] Cosimo Bambi and Andrea Santangelo, editors. *Handbook of X-ray and Gamma-ray Astrophysics*. Springer, 2024.

[21] S. Agostinelli et al. GEANT4: A simulation toolkit. *Nucl. Instrum. Meth.*, A506:250–303, 2003.

[22] A.A. Moiseev, R.C. Hartman, J.F. Ormes, D.J. Thompson, M.J. Amato, T.E. Johnson, K.N. Segal, and D.A. Sheppard. The anti-coincidence detector for the glast large area telescope. *Astroparticle Physics*, 27(5):339–358, June 2007.

[23] W. B. Atwood et al. Design and Initial Tests of the Tracker-Converter of the Gamma-ray Large Area Space Telescope. *Astropart. Phys.*, 28:422–434, 2007.

[24] Xu Pan, Wei Jiang, Chuan Yue, Shi-Jun Lei, Yu-Xin Cui, and Qiang Yuan. Simulation study of the performance of the Very Large Area gamma-ray Space Telescope. *Nucl. Sci. Tech.*, 35(9):149, 2024.

[25] A. A. Moiseev, J. F. Ormes, R. C. Hartman, T. E. Johnson, J. W. Mitchell, and D. J. Thompson. Observation and simulations of the backsplash effects in high-energy gamma-ray telescopes containing a massive calorimeter. *Astropart. Phys.*, 22:275–283, 2004.

[26] S Guatelli, D Cutajar, A B Rosenfeld, B Oborn, and Centre for Medical Radiation Physics. Introduction to the geant4 simulation toolkit. *AIP Conference Proceedings*, 1345(1), 5 2011.

[27] S. Riggi, P. La Rocca, E. Leonora, D. Lo Presti, G.S. Pappalardo, F. Riggi, and G.V. Russo. Geant4 simulation of plastic scintillator strips with embedded optical fibers for a prototype of tomographic system. *Nuclear Instruments and Methods in Physics Research Section A: Accelerators, Spectrometers, Detectors and Associated Equipment*, 624(3):583–590, 2010.

[28] J. et al. Allison. Geant4 developments and applications. *IEEE Transactions on Nuclear Science*, 53(1):270–278, 2006.

[29] J. Allison et al. Recent developments in geant4. *Nuclear Instruments and Methods in Physics Research Section A: Accelerators, Spectrometers, Detectors and Associated Equipment*, 835:186–225, 2016.

[30] V.N. Ivanchenko. Geant4: physics potential for hep instrumentation. *Nuclear Instruments and Methods in Physics Research Section A: Accelerators, Spectrometers, Detectors and Associated Equipment*, 494(1):514–519, 2002. Proceedings of the 8th International Conference on Instrumentatio n for Colliding Beam Physics.

[31] J. Apostolakis and M. Asai et al. Geometry and physics of the geant4 toolkit for high and medium energy applications. *Radiation Physics and Chemistry*, 78(10):859–873, 2009. Workshop on Use of Monte Carlo Techniques for Design and Analysis of Radiation Detectors.